Marine and Petroleum Geology 124 (2021) 104777

Contents lists available at ScienceDirect

Marine and Petroleum Geology

journal homepage: www.elsevier.com/locate/marpetgeo

Research paper

The Messinian Salinity Crisis deposits in the Balearic Promontory: An undeformed analog of the MSC Sicilian basins??☆

Fadl Raad [a,*], Johanna Lofi [a], Agnès Maillard [b], Athina Tzevahirtzian [c], Antonio Caruso [c]

[a] Géosciences Montpellier, CNRS, Université de Montpellier, Université des Antilles - Bâtiment 22, Université de Montpellier 2, Place E. Bataillon, Montpellier Cedex 05, 34095, France
[b] Géosciences Environnement Toulouse (GET), Observatoire Midi Pyrénées, Université de Toulouse, CNRS, IRD, 14 avenue E. Belin, Toulouse, F-31400, France
[c] Dipartimento di Scienze della Terra e del Mare (DiSTeM), Università degli Studi di Palermo, Via Archirafi 20-22, 90123, Palermo, Italy

ARTICLE INFO

Keywords:
Messinian salinity crisis
Balearic promontory
Central Mallorca depression
Caltanissetta basin
Outcrops

ABSTRACT

The Messinian Salinity Crisis (MSC) is a controversial geological event that influenced the Mediterranean Basin in the late Miocene leaving behind a widespread Salt Giant. Today, more than 90% of the Messinian evaporitic deposits are located offshore, buried below the Plio-Quaternary sediments and have thus been studied mainly by marine seismic reflection imaging.

Onshore-offshore records' comparisons and correlations should be considered a key approach to progress in our understanding of the MSC. This approach has however not been widely explored so far. Indeed, because of the erosion on the Messinian continental shelves and slopes during the MSC, only few places in the Mediterranean domain offers the opportunity to compare onshore and offshore records that have been preserved from erosion. In this paper, we compare for the first time the MSC records from two basins that were lying at intermediate water depths during the MSC and in which salt layers emplaced in topographic lows: the Central Mallorca Depression (CMD) in the Balearic Promontory, and the Caltanissetta Basin (CB) in Sicily. The reduced tectonic movements in the CMD since the late Miocene (Messinian) till recent days, favored the conservation of most of the MSC records in a configuration relatively close to their original configuration, thus allowing a comparison with the reference records outcropping in Sicily. We perform seismic interpretation of a wide seismic reflection dataset in the study area with the aim of refining the mapping of the Messinian units covering the Balearic Promontory (BP) and restituting their depositional history based on a detailed comparison with the Messinian evaporitic units of the Sicilian Caltanissetta Basin. We discuss how this history matches with the existing 3-stages chrono-stratigraphic model. We show that the Messinian units of Central Mallorca Depression could be an undeformed analog of those outcropping on-land in the Sicilian Caltanissetta Basin, thus questioning the contemporaneous onset of the salt deposition on the Mediterranean scale. We show a change in seismic facies at a certain range of depth between stage 1 MSC units, and wonder if this could reflect the threshold/maximum depth of deposition of bottom growth PLG selenites passing more distally to pelagic snowfall cumulate gypsum. Moreover, we confirm that PLG could be deposited in water depths exceeding 200 m.

1. Introduction: Messinian Salinity Crisis and intermediate basins

The Messinian Salinity Crisis (MSC) is a prominent and still misunderstood event that influenced the Mediterranean Basin in the late Miocene, leaving behind a Salt Giant with a volume of about 1.2×10^6 km^3 (Ryan, 1976; Haq et al., 2020) deposited in a relatively short time interval of ~0.64 Ma (Krijgsman et al., 1999a,b; CIESM, 2008; Manzi et al., 2013). The first studies dedicated to the MSC took place onshore (Selli, 1960) while offshore works (Ryan et al., 1971) followed the first scientific drillings of the deep-sea drilling project DSDP (Hsu et al., 1973b). Since then and until today, numerous studies have been conducted in order to better understand the series of events that modified the basin during the Messinian and, despite these efforts, most of the controversies still persist (see review in Roveri et al., 2014a). A consensus model for the MSC was proposed after the CIESM publication

☆ SaltGiant: www.saltgiant-etn.com

* Corresponding author. Department of Geosciences Montpellier, France.
E-mail address: fadl.raad@umontpellier.fr (F. Raad).

https://doi.org/10.1016/j.marpetgeo.2020.104777
Received 18 June 2020; Received in revised form 16 October 2020; Accepted 18 October 2020
Available online 24 October 2020

in 2008, inspired from the 2 stage model of Clauzon et al. (1996), where the MSC has been divided in 3 stages:

- stage 1 (from 5.97 to 5.60 Ma, i.e. ~370ky): this stage marks the MSC onset, where the lowermost primary evaporites were deposited in shallow water basins.
- stage 2 (from 5.60 to 5.55 Ma, i.e. ~50ky): at this stage, salt bodies (mainly halite) were deposited in deep basins accompanying the maximum sea-level drawdown (of debated amplitude). Shallower basins evaporites underwent erosion and reworked evaporites were deposited.
- stage 3 (from 5.55 to 5.33 Ma, i.e. ~220ky): this stage was later on divided into 2 sub-stages, stage 3.1 (from 5.65 to 5.42), in which upper evaporites were emplaced and stage 3.2 (from 5.42 to 5.33), that is known also as Lago Mare stage, where sediments with brackish water fauna content were deposited.

This model has been widely built based on onshore studies performed on several key peri-Mediterranean outcrops among which the ones from Sicily. This model has recently been challenged at least for the Eastern Mediterranean Basins by studies from recent oil industry offshore drillings (e.g. Meilijson et al., 2019).

Today, more than 90% of the MSC evaporites are lying offshore (Fig. 1A; Ryan et al., 2009; Lofi et al., 2011a, b; Lofi, 2018). Offshore drillings remain very limited (DSDP and ODP drillings and oil industry wells) and the offshore MSC records thus still largely un-sampled. The most efficient approach in the offshore domain remains the seismic reflection method.

There is an agreement about the important role of the pre-MSC topography on the distribution of the MSC sediments, although paleogeographic reconstructions are still not well constrained (Mascle and Mascle, 2019). In their review, Roveri et al. (2014a) proposed a schematic classification of the Messinian sub-basins in the Mediterranean, where they differentiate shallow (0–200 m water depth), intermediate (i.e. relatively deep-water, 200–1000 m) and deep basins (water depth $>$ 1000 m). In this view, these sub-basins are thought to be physically disconnected from each other by topographic sills, and hold specific MSC records.

The shallow marginal basins have been largely studied onland as they are outcropping in areas tectonically active during and/or after the MSC (e.g. Southeastern Spain, Apennines, Piedmont).

The Messinian sedimentary record in these basins is nevertheless always incomplete because it has been exposed to erosion during the MSC sea level fall and/or due to tectonics. The main feature in the onshore outcrops is the presence of thick gypsum beds that mark the onset of the MSC (e.g. Yesares member in Sorbas Basin (Krijgsman et al., 2001); Vena del Gesso formation in the Northern Apennines (Vai and Lucchi, 1977); Cattolica Gypsum group in the central Sicilian Basin (Decima and Wezel, 1971)). They are called Primary Lower Gypsum (PLG), corresponding to MSC stage 1 and are usually interpreted as

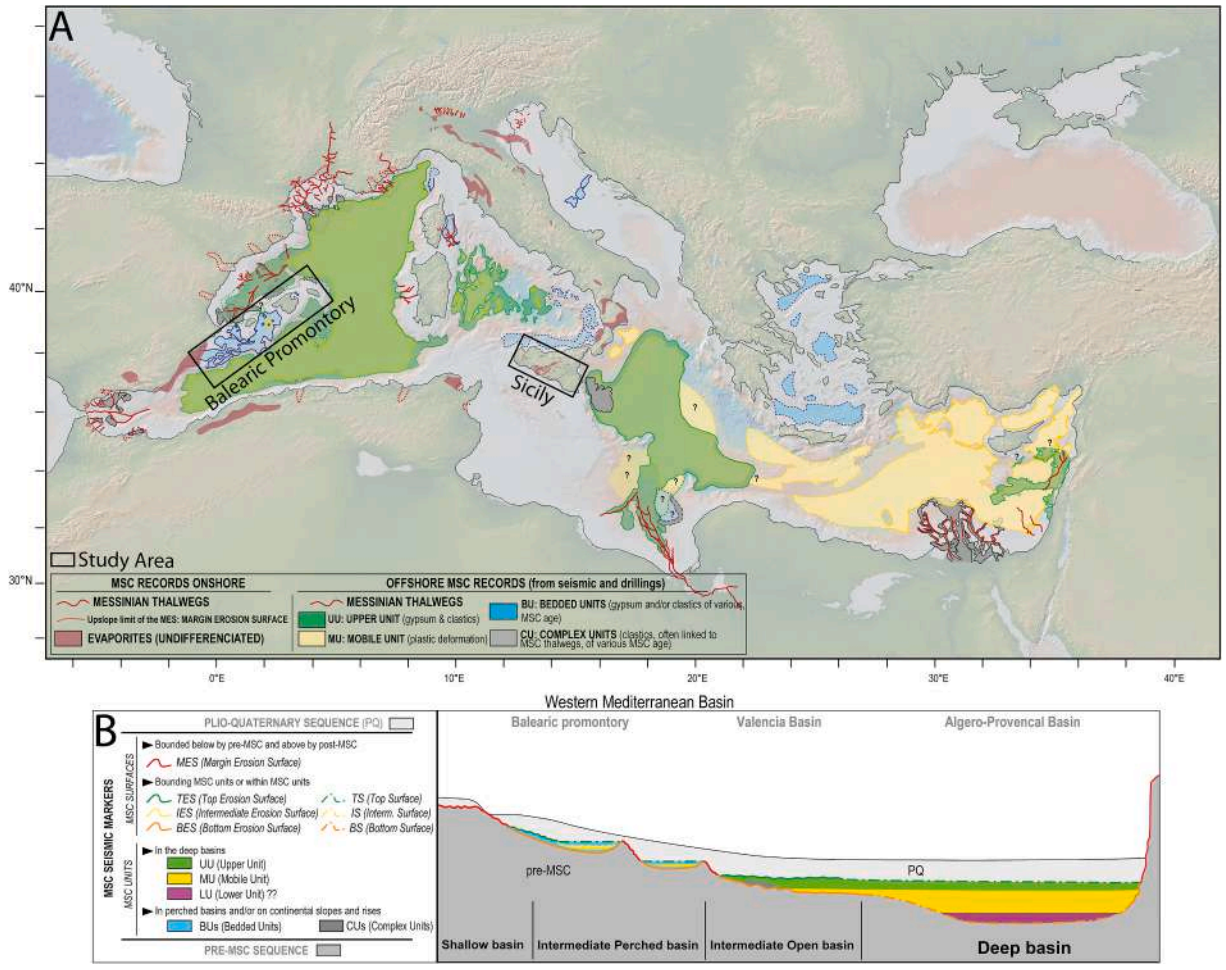

Fig. 1. A: Extension map of the MSC seismic units around the Mediterranean illustrating our study area (modified from Lofi, 2018). Relief map is taken from Geomapapp (www.geomapapp.org). B: schematic present-day cross section of the Western Mediterranean basin. It shows a conceptual present-day distribution of the MSC offshore markers along a transect from shallow into deep basin passing through the intermediate basin (salt tectonics and post MSC movements are not included) (modified from Lofi, 2018).

precession driven beds (Lugli et al., 2010). A few studies have also recognized the presence of PLG in the offshore domain (e.g. Northern Adriatic Sea (Ghielmi et al., 2013); Balearic Promontory (Ochoa et al., 2015)).

The deep MSC basins are only observed offshore and they contain salt sequences >1 km thick (see review in Lofi et al., 2011a, 2011b; Lofi, 2018). In the Western Mediterranean, the Algero-Provencal Basin is known to contain the full MSC sedimentary sequence or the so-called trilogy (Montadert et al., 1970).

Following the nomenclature of Lofi et al. (2011a,b), the 3 main seismic units forming this deep basin succession are: 1- the lower unit (LU), never sampled; 2- the mobile unit (MU), thought to be mainly made of Halite based on its transparent seismic facies and plastic deformation; 3- the upper unit (UU) which uppermost part is made of clastic sediments, dolomitic marls, clastic gypsum and anhydrite (Hsu et al., 1973a). The deep basin trilogy of the western Mediterranean Basin has never been drilled except for its topmost part, and thus lacks chronostratigraphic and lithostratigraphic control. The MSC record in the eastern Mediterranean (Levant Basin) differs from the trilogy described in the western basin (Lofi et al., 2011a, b; Lofi, 2018) as it consists of up to 2 km thick halitic MU with distinct internal reflection packages (Bertoni and Cartwright, 2006; Feng et al., 2016; Meilijson et al., 2019), overlain by a thin UU (Gvritzman et al., 2017; Madof et al., 2019) made of clastic rich anhydrite that has been recently drilled (Gvritzman et al., 2017).

The intermediate basins are lying between the shallow and deep basins (e.g. Cyprus and Caltanissetta Basins). The MSC record in these basins differs from the one described in shallow (containing mainly PLG) and deep (thick salt layer) basins, and can contain various deposits: 1- euxinic shales/dolostones of stage 1 that are considered the later distal equivalent of the PLG (e.g. Piedmont Basin (Dela Pierre et al., 2011)), 2- Resedimented Lower Gypsum RLG of stage 2 (e.g. Sicily (Roveri et al., 2006)) and 3- Upper Evaporites UE of stage 3 (e.g. Cyprus (Manzi et al., 2016)).

When lying offshore today, intermediate basins can also contain various seismic units that are Messinian in age, including 1- bedded units (BU) (e.g. Balearic promontory (Driussi et al., 2015; Maillard et al., 2014); Adriatic Basin (Ghielmi et al., 2013); Eastern Corsica Basin (Thinon et al., 2016)), 2- a relatively thin salt layer (e.g. Balearic Promontory (Maillard et al., 2014)), and 3- an UU (e.g. Valencia Basin (Maillard et al., 2006)) lying above a Complex Unit (CU) (Valencia Basin (Cameselle and Urgeles, 2017)).

In this work, we consider as intermediate any basin that during the MSC was lying deeper than marginal basins (~200 m water depth) and shallower than the deep basins, containing either none of the deep basin MSC trilogy members or only some of them (Fig. 1B).

Some or part of the intermediate basins are outcropping nowadays (e.g. Sicily and Mesaoria Basins) and are thus considered as key areas to provide a stratigraphic link between marginal and deep basins. Offshore intermediate basins have not been intensively studied so far, although they may permit a comparison with some key onshore outcrops. Another importance of the offshore intermediate basins is that they may contain sedimentary records that are missing in the onshore outcrops that have undergone post-MSC erosion.

In this paper, we compare two basins that are thought to be lying at intermediate depths during the MSC and in which salt layers are encountered: the Central Mallorca Depression (CMD) on the Balearic Promontory (Maillard et al., 2014), and the Caltanissetta Basin (CB) in Sicily (Roveri et al., 2014b). The first one is lying offshore between Ibiza and Mallorca islands, in a passive tectonic setting, and is studied via seismic profiles. The second one is lying onshore in an active tectonic context, and its outcrops have been studied widely as references for understanding the MSC. First, we present a detailed study of the seismic records of the CMD. We then discuss similarities, in terms of geometry, facies, distribution and thickness between the Messinian deposits in both basins and we attempt to demonstrate that the CMD may be considered as an undeformed analog of the Sicilian CB. Finally, we propose a depositional scenario for the CMD and discuss the implications of the observations on the MSC event.

2. Geological background of the study areas

2.1. The Balearic Promontory: Tectonics, architecture and Messinian Salinity Crisis

Surrounded by 2 deeper basins, the Balearic Promontory (BP) is a continental high that includes the Balearic Islands. It is made of 2 main morphologic blocks (Acosta et al., 2002): the Mallorca-Menorca block and the Ibiza-Formentera block (Fig. 2). The two blocks are separated by an elliptical depression, approximately 1050 m water deep, called the Central Mallorca Depression (CMD). To the south, the BP is delimited by 2 steep escarpments marking the border with the Algero-Provencal deep Basin (>2400 m depth): the Mazarron and Emile Baudot Escarpments, separated by the Ibiza Channel that, with the Mallorca Channel, connects the BP to the Valencia Basin (>1200 m depth) (Fig. 2).

The BP is known to be the north-eastern prolongation of the compressional Betic Cordillera thrust system (Roca, 2001). It is thought that the compression started in the late Oligocene to the south and then prolongated further to the north during the Burdigalian (Gelabert et al., 1992; Sabat et al., 2011), while the surrounding Valencia and Algerian Basins underwent rifting in the back-arc context of the retreating Apennines-Maghrebian subduction. From late Serravallian and up to recent times, the BP underwent mild post-orogenic extension, resulting in a NE-SW normal fault system expressed plainly by the Palma Graben in Mallorca (Roca and Guimera, 1992; Sabat et al., 2011).

This tectonic evolution of the BP thus resulted in a very complex structure including highs and lows resulting from compression and extension. The present-day BP contains a series of perched sub-basins lying at different depths, stepped from the present-day coastline near Alicante (Spain) down to the deep basin (Fig. 3A and B). Most of these sub-basins were probably already existing during the Messinian and inherited their structure from the tectonic evolution of the promontory. Today they are forming a series of topographic lows (Fig. 3B), more or less connected, lying at various water depths (Driussi et al., 2015). During the MSC, these lows have been filled with deposits up to 500 m thick (Maillard et al., 2014; Driussi et al., 2015; Ochoa et al., 2015).

2.1.1. MSC in the surrounding deep basins

South of the BP, the MSC record in the Algerian Basin is represented by the deep basin trilogy ie. LU, MU and UU (Lofi et al., 2011a, b; Lofi, 2018). The UU and MU pinch out on the Mazarron and Emile Baudot escarpments (Camerlenghi et al., 2009) and they show no connection with the MSC units of the BP (Figs. 3A and 4A). North-East of the BP, in the Provencal Basin, the MSC trilogy is also present (Montadert et al., 1970; Lofi et al., 2005). Towards the Valencia Basin, the LU and MU thin out progressively and pinch out in the area where a volcanic ridge separates the Provencal from the Valencia Basin (Fig. 3A; Maillard and Mauffret, 2006; Maillard et al., 2006; Pellen et al., 2019). The UU extends into the Valencia Basin, thinning out from the NE to the SW where it pinches out and passes into a Margin Erosional Surface (MES) on the Catalan/Ebro Margins and volcanic structures (Maillard et al., 2006; Urgeles et al., 2011), whereas towards the east it drapes the lower margin of the BP (Driussi et al., 2015) and it passes into a MES. In the western extremity of this basin, Cameselle et al. (2017) evidenced the existence of a widespread CU unconformably overlain by, here very thin, UU (Fig. 3A). They interpreted the CU as mass transport deposits resulting from large-scale destabilization of the continental slope during the initial rapid sea-level drawdown and exposure of the shelf and upper slope. Other CU exist locally at the downslope mouth of Messinian valleys (Maillard et al., 2006)

Recently, Pellen et al. (2019) interpreted an additional MSC unit (unit SU12) lying below the MES on the Ebro Margin, and below the LU

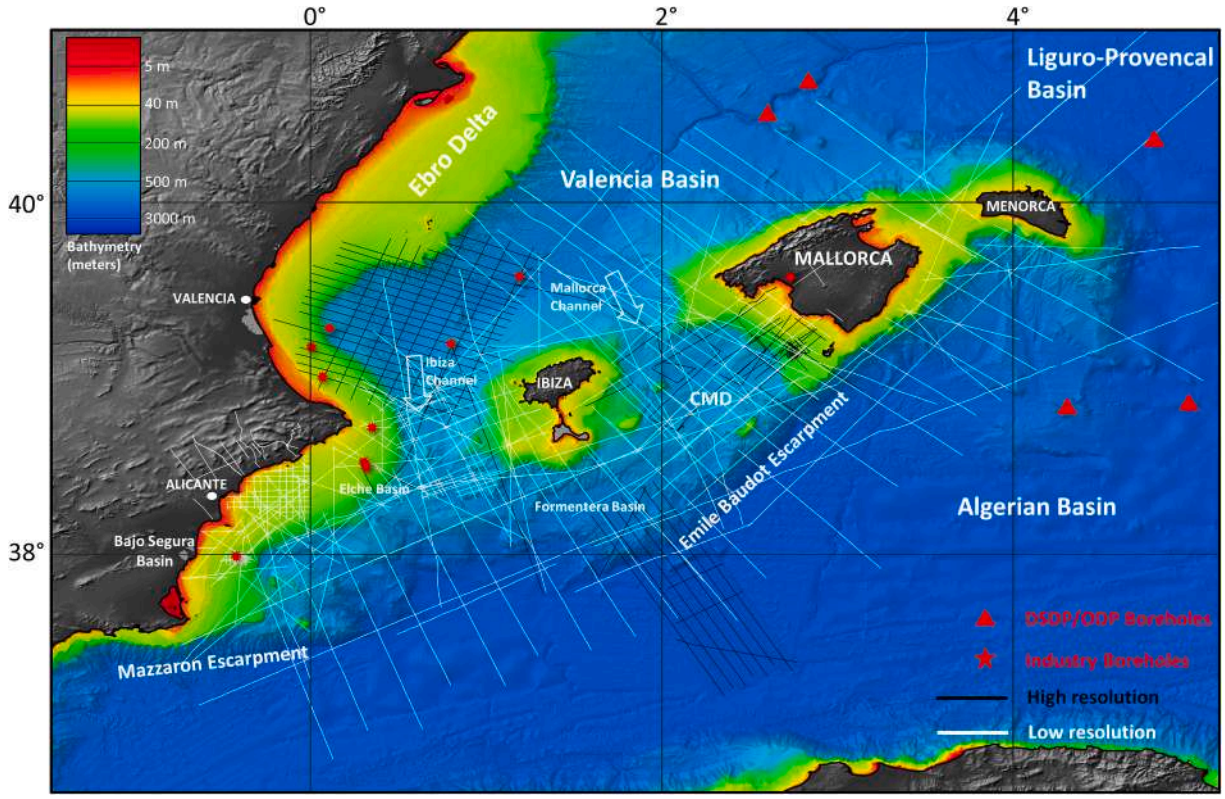

Fig. 2. Bathymetric map showing the seismic dataset used for this study. CMD= Central Mallorca Depression. Bathymetry is downloaded from the European Marine Observation and Data network (EMODnet) database available online (www.emodnet-bathymetry.eu). White thick arrows indicate marine channels. Boreholes shown in the map represent a set of both industrial (IGME) and exploratory drillings (ODP and DSDP). Onshore digital elevation model has been produced using Copernicus data and information funded by the European Union- EU-DEM layers (www.eea.europa.eu).

in the Valencia and Provencal Basins, which is thought to have been deposited during the MSC base-level fall. Maillard et al. (2006) proposed that following this important base level drop, the Valencia Basin was subaerially exposed and a widespread erosion surface was created (Bottom Erosional Surface, BES). The UU successively was emplaced under shallow water during a relative rise in base level as attested by their aggrading and onlapping geometry (Lofi et al., 2011a, b). An erosional surface at the top of the UU (Top Erosional Surface, TES) could be a result of dilution during the Lago-Mare phase, possibly associated to a base level drop preceding the Zanclean reflooding (Escutia and Maldonado, 1992; Maillard et al., 2006). For Camesselle and Urgeles (2017) this erosion is minor and can be found only locally due to the dilution during the Lago Mare event.

2.1.2. *MSC in the Balearic Promontory*

Several studies showed the presence of a thin MSC unit offshore the BP, disconnected from the other MSC units in the surrounding basins (Maillard et al., 2014; Driussi et al., 2015; Ochoa et al., 2015). Based on seismic profile interpretation, Driussi et al. (2015) identified a "MSC unit" (Table 1) extending all over the BP (their Fig. 4) from the present-day coastline down to the deepest part in the Formentera Basin (~1750 m). This seismic unit is characterized by 2–7 sub-parallel continuous reflections of medium amplitude. It locally includes an internal facies made up of very thin reflections (Ft) with lower amplitude, found usually at the top of the MSC unit. The "MSC unit" is locally lying on an erosional unconformity (BES) and is eroded at the top (TES) towards the borders of the CMD.

Several works then proposed that this "MSC unit" is made of several sub-units and that not all of them have the same MSC age, depending on their location on the promontory (Maillard et al., 2014; Ochoa et al., 2015; Roveri et al., 2019).

Ochoa et al. (2015), based on borehole cuttings and logs tied to high-resolution seismic reflection profiles, demonstrated that the "MSC unit", which they called Bedded Unit (BU, sensu Lofi et al., 2011a, b) (Table 1), in Elche and Bajo Segura sub-basins corresponds to the PLG (Fig. 3B; see also their Figs. 2 and 8). This PLG is equivalent to the first stage evaporites found onland, for example in the Sorbas and Bajo Segura Basins (Soria et al., 2008) or in the Palma Basin boreholes (Fig. 4A; Baron and Gonzalez, 1985; Rosell et al., 1998; Maillard et al., 2014; Garcia-Veigas et al., 2018). In this area, the seismic facies of the PLG consists of sub-parallel continuous 2 to 7 reflectors forming a Bedded Unit (BU), with very strong acoustic impedance at the base and at the top (see their Fig. 8). It is clearly cut by the TES, whereas no erosion is identified at the bottom. Based on their results, these authors suggested that PLG gypsum precipitation and/or preservation could occur in non-silled basins at water depth exceeding 200 m. Both Ochoa et al. (2015) and Driussi et al. (2015) questioned the connectivity between the different shallow sub-basins (e.g. Bajo Segura and Elche Basins) and the ones currently lying deeper, because of the presence of local structural highs separating them, and because the density of seismic profiles is not high enough to show the connectivity. More recently, Roveri et al. (2019) hypothesized that only the shallower domains of the Elche and Bajo Segura sub-basins contained PLG, with the deeper parts of these basins located beyond some volcanic sills containing Resedimented Lower Gypsum (RLG) (their Fig. 14 a, b). However, no data support their new interpretation and mapping. At the present time, it is thus not clear whether the BUs filling the sub-basins lying deeper correspond to PLG, RLG or another MSC deposit.

In a study dedicated to the CMD, Maillard et al. (2014) distinguished two different sub-units within the MSC unit of Driussi et al. (2015) (see their Fig. 7): 1- a Slope Unit (SU) located clearly on the Mallorca and Ibiza slopes and 2- a Bedded Unit (BU) lying deeper and containing a thin salt unit (Table 1). The authors discussed the possible chrono-stratigraphic models for those 2 MSC units in the CMD (see their

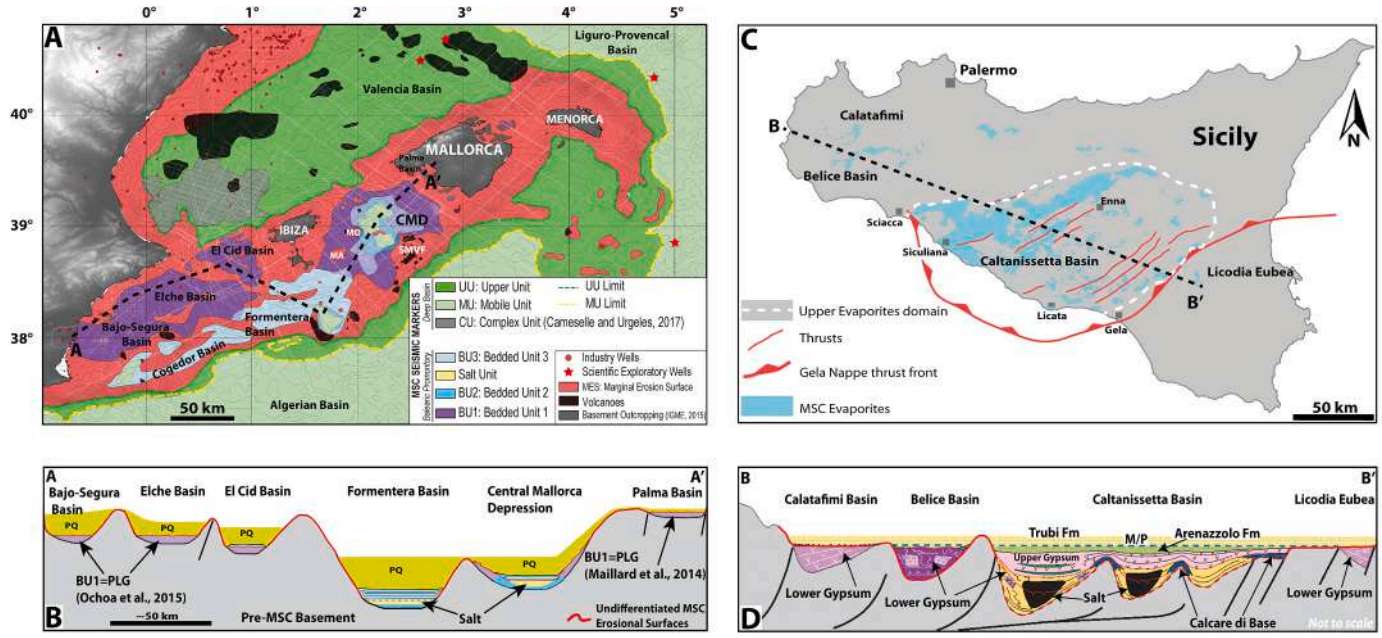

Fig. 3. A: Map showing the present-day extent of the MSC units in the Balearic Promontory (BP) and the surrounding deep basins. Light grey lines are isochrones (every 200 ms TWTT) of the offshore depth of the base Plio-Quaternary unit. Black dotted line shows the position of the section shown in 3 B. Thin white lines in the background are the positions of the seismic profiles used for the interpretation. MA = Mount Auzias; MO = Mount Oliva; SMVF=South Mallorca Volcanic Field; CMD=Central Mallorca Depression. Note that on the BP salt units are present in different perched basins (CMD, Cogedor Basin and Formentera Basin) lying at different depths. Notice also that bedded unit (BU1) extension in Elche and Bajo Segura basins is more important than what has been mapped by Driussi et al. (2015). B: Schematic profile across the perched basins of the BP showing the present day setting of the different bedded and salt units overlain by the PQ unit; the colors of the MSC units are the same used in 3 A's legend. The pre-MSC basement was drawn from the compilation and mapping of the Base Messinian horizon from the seismic dataset. Black dotted line shows the position of the section shown in 3D. PQ= Pliocene-Quaternary unit. C: Simplified map of the extent of the MSC evaporitic sediments in the different Sicilian basins (modified from Caruso et al., 2015). D: Schematic geological cross section across the Sicilian MSC basins showing the settings of the evaporitic units filling the sub basins topped by the base Pliocene Trubi sediments (modified from Roveri et al., 2006). Notice how in both the BP and Sicilian basins, the different sedimentary units belonging to the MSC are contained in a series of sub-basins lying at different depths with only the deepest basins containing salt. (For interpretation of the references to color in this figure legend, the reader is referred to the Web version of this article.)

Fig. 12). They question whether the SU, being older than the BU, could be synchronous or could post-date the emplacement of the PLG of the Palma Basin. Based on low-resolution high-penetrative seismic profiles, Maillard et al. (2014) also argued that the salt layer in the CMD might be thicker than what is observed on the high-resolution seismic lines. Another salt unit is recognized in the southernmost part of Formentera sub-basin (Fig. 3A and B and Fig. 5D; Driussi et al., 2015). It is lying on a present-day depth of ~450 m below seafloor, whereas the salt in the CMD lies on 520 m below seafloor.

Onland Mallorca, the MSC record is expressed by the Santanyi limestones, that represent the Terminal Carbonate Complex (TCC), made of carbonatic microbialites, oolites and marls (Mas Gornals and Fornós Astó, 2012). These authors suggest that the TCC is the lateral time equivalent of the PLG drilled in the bay of Palma. None of the boreholes drilled onland Mallorca records the TCC and PLG together (Baron and Gonzalez, 1985), which supports this interpretation. Overlying the TCC, and below the lower Pliocene sediments, there is a lacustrine-continental sedimentary unit known as the Ses Olles Formation that contains brackish to fresh water faunal assemblages, thus interpreted as representing the Lago Mare episode (Mas and Fornos, 2013). According to these authors the Lago Mare unit is cut by an erosional surface created during the major base-level drawdown, suggesting that the Lago Mare phase is related here to stage 1 of the MSC. This is not in agreement with the current crono-stratigraphic model (CIESM, 2008; Roveri et al., 2014a).

Onland Ibiza, Late Miocene units outcrop only locally and show common characteristics with units known in Mallorca, such as the reef complex or a unit interpreted as the TCC (Durand-Delga et al., 1993; Pomar et al., 1996; Lezin et al., 2017). Important continentalization episode has been recently identified on top of these units with erosion and karstification, paleosols and gravity-driven instabilities that are thought to record the major sea-level fall (Odonne et al., 2019; Maillard et al., 2020).

2.2. *The Sicilian central Caltanissetta Basin: Geological context and MSC*

Unlike the BP, the Sicilian Basins have been very active tectonically since the MSC.

Belonging to the Central Mediterranean domain, Sicily's structural and geological evolutions derive from the convergence between the African continental margin and the Eurasian plate (Catalano et al., 2013; Henriquet et al., 2020).

During the lower Miocene, the SE-wards shift of the Calabrian accretionary wedge above the slab, including AlKaPeCa blocks (i.e. Alboran, Kabylies, Peloritani, Calabria; Bouillin, 1986), lead to the growth of the Sicilian collisional complex (Catalano et al., 1996). The latter corresponds to a well-exposed fold-and-thrust belt (FTB) (Albanese and Sulli, 2012), the Maghreb-Apennine thrust belt, crossing from east to west the Sicily Island with the Gela Nappe along the thrust front (Lickorish et al., 1999).

The Caltanissetta Basin, located in the arcuate part of the Gela Nappe (Fig. 3C), represents the main foredeep of the frontal thrust belt system (Butler and Lickorish, 1997). It consists of a single thrust sheet and comprises a series of continuously tightening folds (Lickorish et al., 1999). Its late Neogene evolution is related to the opening of the Tyrrhenian Sea (Kastens et al., 1988). The CB is organized in an alternation of depocenters and highs that are mostly related to active thrusting synclines (Grasso and Butler, 1991; Butler et al., 1995; Catalano et al., 2013).

During the MSC, evaporites including halite were deposited in the CB

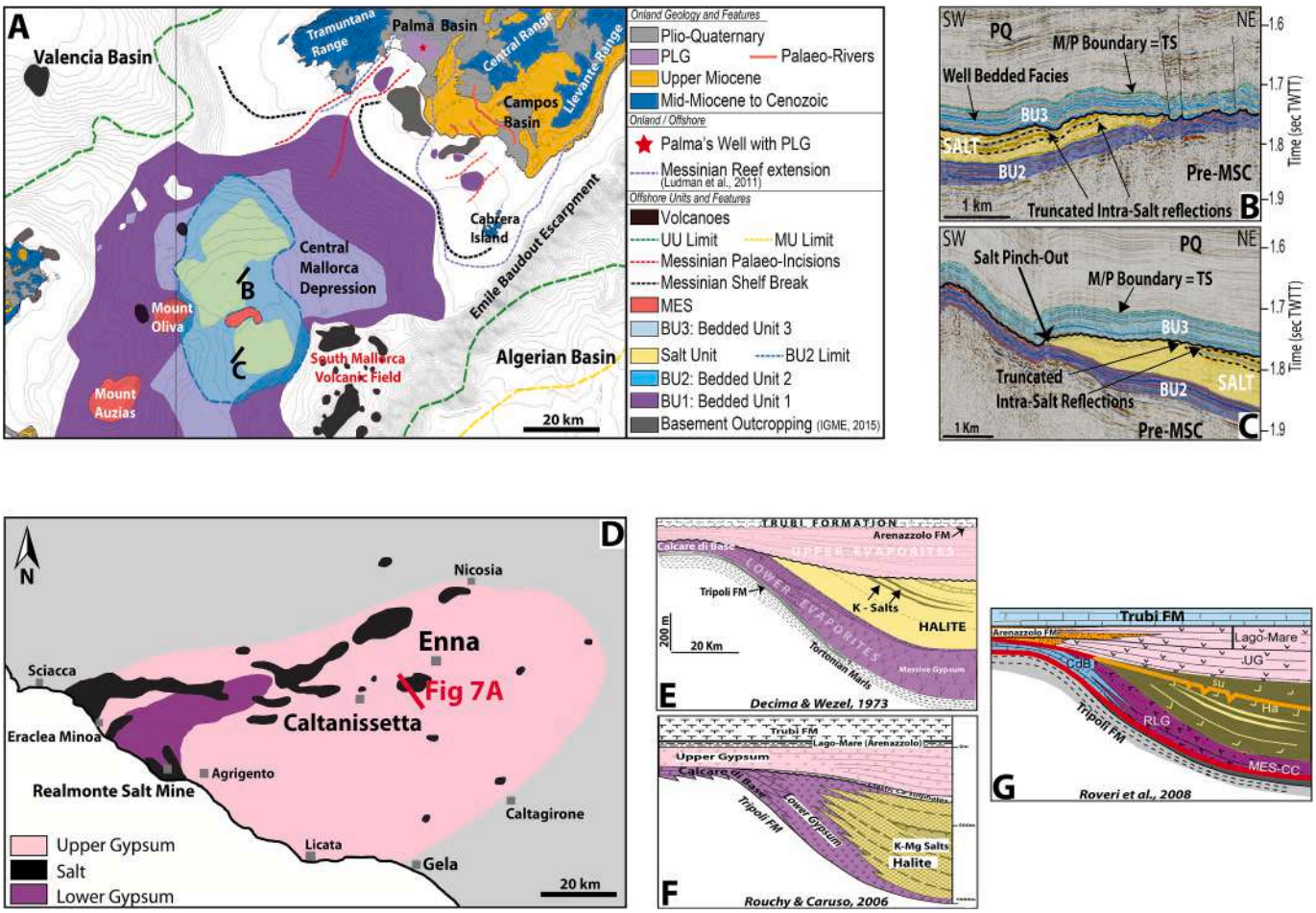

Fig. 4. A: Detailed map of the MSC units and features in the Central Mallorca Depression (CMD). Note how the salt in the depocenter of the depression is distributed in 2 patches separated by a local topographic high. Isobaths (every 50 m) represent the present-day bathymetry. Onland geology mapping of south Mallorca and North Ibiza is modified from geological map of Spain 1:50000 (IGME). Volcanoes and outcropping basement are from the geological map of Spain 1:1,000,000. BU1-PLG unit in the Palma Basin is mapped after Maillard et al. (2014). B–C: Parts of seismic profiles illustrating the geometrical relationship between the MSC units in the CMD: they show how the salt is lying between two MSC bedded units (BU2 and BU3) and contains internal reflections truncated at the top by an erosional surface. D: Map showing the distribution of the evaporitic units in CB (modified from Caruso et al., 2015). E–G: Sedimentary models showing the settings and geometrical relationships of the MSC evaporites in the CB published by different authors since the beginning of the studies of the MSC in that area (modified from Decima and Wezel, 1973; Rouchy and Caruso, 2006, Roveri et al., 2008). Note how in both study areas the settings and the geometrical relationships between the sedimentary units are similar, where we have a salt unit eroded at the top and sandwiched between two other units belonging to the MSC.

Table 1
Synthesis of the Messinian units in the Balearic Promontory from all the offshore studies dedicated to the MSC.

Lofi et al. (2011a, b)	Maillard et al. (2014)	Driussi et al. (2015)	Ochoa et al. (2015)	Roveri et al. (2019)	This study
BU	BU Salt SU	Ft Salt MSC unit	BU Salt BU - PLG	BU - RLG Salt BU - PLG	BU3 Salt BU2 BU1

and are mostly outcropping today, which made it a reference basin for the study of the MSC event. A complete sequence has been also found in a great number of cores in the CB, where the sequences are schematically formed of Tripoli Formation (30–90 m), Calcare di base alternated to primary selenitic gyspum (>300 m), halite and kainite (~500 m) and Upper Gypsum (100–200 m) (Rouchy and Caruso, 2006; Caruso et al., 2015). This tripartite character of the MSC sequence recalls the deep basin trilogy, thus the MSC succession of the central Sicilian CB was initially analogized to an uplifted part of the deep basin succession, although not necessarily as the deepest areas (Decima and Wezel, 1971; Garcia-Veigas et al., 1995; Hsü et al., 1978; Rouchy, 1982a; Rouchy and Saint Martin, 1992; Schreiber, 1978; Clauzon et al., 1996; Rouchy and Caruso, 2006). However, different opinions exist about the marginal vs. deep basinal character of Sicily during the Messinian (Clauzon et al., 1996, 2005; Krijgsman et al., 1999a,b; Butler et al., 1995) which resulted in a number of chrono-stratigraphic models and related MSC scenarios (Fig. 4 E-G; e.g. Decima and Wezel 1971; Garcia Veigas et al., 1995; Butler et al., 1995; Rouchy and Caruso 2006; Roveri et al., 2008). Recently, some authors classified the CB as an intermediate basin with a complex stratigraphy as a result of its growth on an orogenic wedge (Roveri et al., 2008, 2014b).

According to the mentioned works, the MSC deposits in CB (Fig. 4D) can be summarized as follows:

- **Lower Evaporites (LE) or Lower Gypsum (LG)** (Decima and Wezel, 1973): this unit is made of massive bedded gypsum intercalated with clay beds with a thickness up to 140 m (Lugli et al., 2010). Roveri et al. (2006) divided this unit into primary PLG and resedimented RLG. The PLG consists of thick selenitic gypsum beds that vary from large massive selenites to gypsarenites, separated by thinner organic-rich shale horizons. The change in facies inside each cycle is thought to reflect the passage from arid to humid phase at the

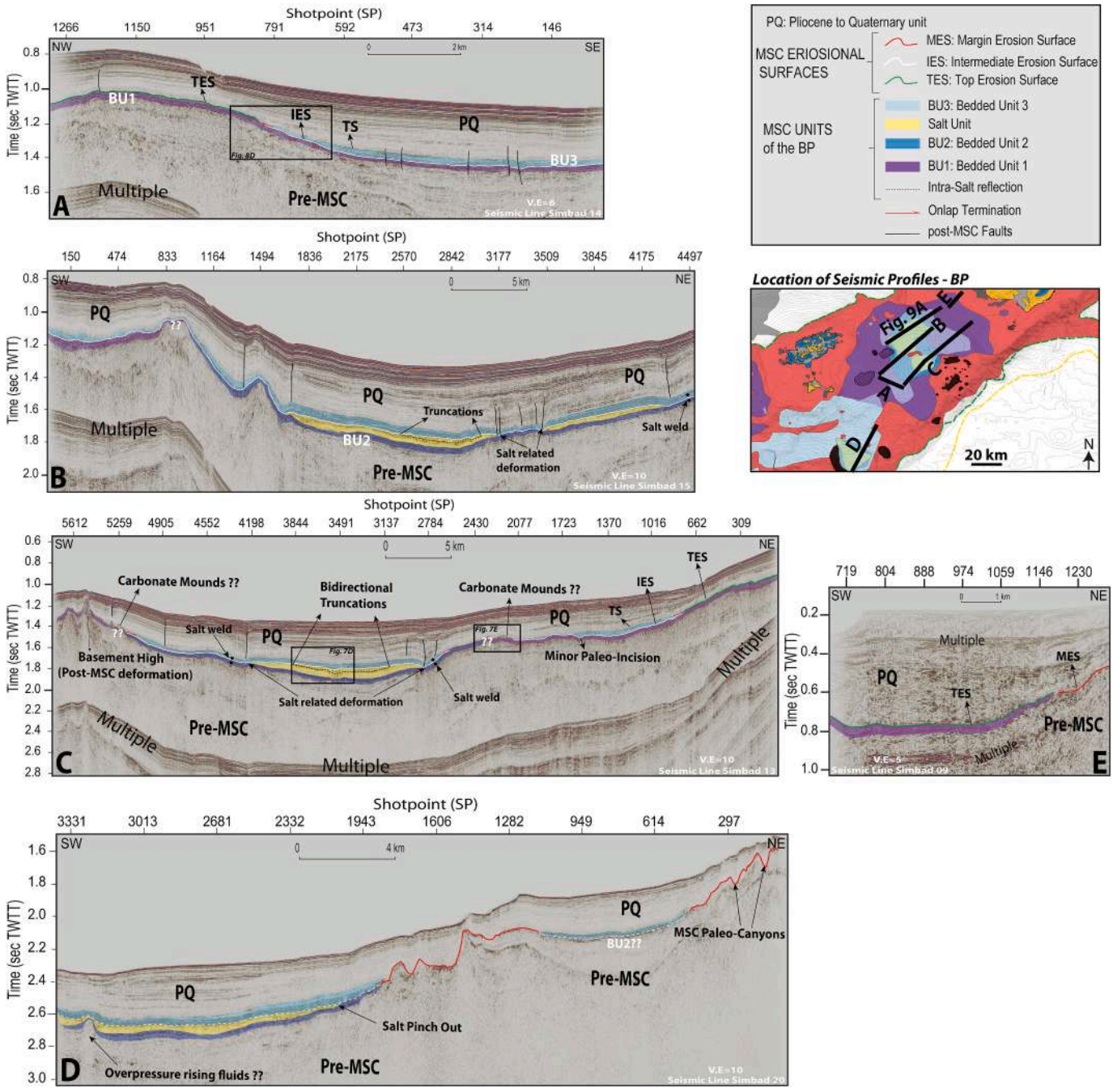

Fig. 5. Seismic profiles covering different parts in the BP area. A: interpreted seismic profile Simbad 16 imaging the MSC seismic units in the southern part of the CMD, at the base of the Ibiza slope, where BU3 onlaps BU1. B–C: Interpreted seismic profiles Simbad 15 and Simbad 13 crossing the depocenter of the CMD showing all the MSC units and erosional surfaces. Note the bilateral truncation of the internal reflections intercalated in the salt unit due to an erosional event. D: Interpreted seismic profile in the southern depression of the Formentera Basin showing the presence of salt lying between 2 bedded units. E: Part of interpreted seismic profile Simbad 09 showing the thinning of BU1 passing into a Marginal Erosional Surface (MES) on the present-day southern shelf of Mallorca.

insolation minima and the insolation maxima respectively at a precessional scale (Lugli et al., 2010). The PLG in the Sicilian MSC basins (Fig. 6A–C) records the same cyclicity (up to 13 cycles; Fig. 6C) as other PLG found in other marginal basins such as Sorbas Basin and the northern Apennines. According to Lugli et al. (2010) the cyclicity encountered in the PLG reflects the paleo-depositional environment, suggesting a general shallowing-upward trend with a change in the general hydrology of the basin. Moreover, these authors state that in the Sicilian Basins, PLG is found exclusively in silled shallow basins (<200 m depth) at the borders of the main foredeep depression and has been deposited during stage 1 of the MSC (CIESM, 2008), whereas the lateral equivalent of the PLG in the deeper parts of the basins is represented by levels of marls, diatomites and thin laminated dolostone (calcare di base 2, see next paragraph) ~20 m thick (Manzi et al., 2011). The base of the PLG unit is conformable with pre-MSC deposits, whereas its top is cut by an erosional surface (Fig. 6A–C). The RLG, bounded by the regional MES at the bottom (Roveri et al., 2008), is found in the main foredeep. It consists of resedimented gypsum that varies from huge and undeformed PLG blocks to gypsarenites and gypsum laminates that has been re-deposited during stage 2 of the MSC. There is a controversy of whether the origin of the RLG is related to the combination of salt

deformation followed by collapse dissolution (Rouchy and Caruso, 2006) or due to sub-aqueous gravity flows in the foredeep due to erosion or thrusting of large PLG masses (Roveri et al., 2008).

- **Calcare di Base (CdB):** this unit is made of complex carbonate formation with different facies (Decima et al., 1988; Rouchy and Caruso, 2006; Ziegenbalg et al., 2010) that are found most commonly on structural highs separating perched basins. The most widespread facies are m-thick micritic limestones (calcite and/or aragonite) of evaporative and/or bacterial origin, often found as brecciated deposits and interbedded with shales and clastic gypsum (Caruso et al., 2015; Perri et al., 2017). The CdB shows common unfossiliferous and evaporitic character marked by halite and gypsum pseudomorphs (Ogniben, 1957; Pedley and Maniscalco, 1999), which suggest a shallow depositional environment close to the coastline (Suc et al., 1995a; Butler et al., 1999). However, the origin and the position of the carbonates belonging to the CdB is still very highly debated. Caruso et al. (2015) consider the CdB as the lateral equivalent to the PLG, slightly diachronous, thus formed during stage 1 of the MSC. These authors argue that the transition from the pre-MSC sediments (Tripoli Formation) to the CdB is continuous without any evident unconformity and they relate the brecciation process observed to local collapses with limited transport. On the other hand, Manzi et al. (2011) divided the CdB into 3 different types, with only type 2 (primary dolomitic limestones) belonging to the first stage of the MSC. Whereas CdB types 1 and 3 belong to the second stage of the MSC, with type 1 formed as the diagenetic product of bacterial sulfate reduction (BSR) of original clastic gypsum in presence of hydrocarbons, and type 3 made of brecciated limestones that formed due to regional mass transports.
- **Salt:** this unit is made mainly of halite and even large amounts of K–Mg salts and it is found mainly in the central CB (Fig. 4D), where its thickness reaches 400–600 m at the Realmonte mine (Decima and Wezel, 1971, 1973; Lugli et al., 1999). There, it shows a clear shallowing upward trend until reaching an exposure surface (Fig. 4E–G and 7B) expressed by ~1.5 m desiccation cracks (Lugli et al., 1999), which suggest that the salt deposition started in a deep stratified water body that experienced a drawdown until the subaerial exposure and truncation (Schreiber et al., 1976; Lugli et al., 1999). It is also characterized by a very high frequency halite-clay cyclicity (cm to dm thick) that has been correlated to Quasi-Biennial Oscillation, the El Nino Southern Oscillation, the sunspot number solar cycle and lunisolar tidal cycle (Manzi et al., 2012). The precession cycles of the deep basin salt of the eastern Mediterranean suggested by Manzi et al. (2018) and more recently by Meilijson et al. (2019) have not been observed in the salts of the CB.
- **Upper gypsum (UG) or Upper evaporites (UE):** like the salt, this unit is present mainly in the CB (Fig. 4D) where it can reach thicknesses up to 300 m. The most complete section outcrops at Eraclea Minoa along the south-western coast of Sicily (Fig. 8C). It is made of a rhythmic alternation of clays and marls interbedded with sandy and fine grained carbonates and seven gypsum bodies made by multiple strata of finely-laminated gypsum (balatino) and gypsarenites/selenites (Caruso and Rouchy, 2006; Grossi et al., 2015). The chrono-stratigraphic tuning of the UE differs between the different authors. Rouchy and Caruso (2006) recognized 6 precession-driven sedimentary cycles, with a possible 7th basal cycle, represented by a deformed gypsum deposit overlaid by the Arenazzolo sandstones (see next paragraph, Arenazzolo member). The Arenazzolo/Trubi contact marks the Messinian/Zanclean boundary (GSSP at Scala dei Turchi - Eraclea Minoa) and the return to normal marine conditions (Van Couvering et al., 2000; Pierre et al., 2006). Whereas Manzi et al. (2009) interpreted nine to ten sedimentary cycles, including the Arenazzolo member. According to these authors, each one of the cycles reflects oscillations in the basin's base level and its water concentration associated to transitions from wet to dry environments, marked by an erosional surface at the end of each cycle. However, there is a disagreement about whether these oscillations started with brackish conditions (e.g. Decima and Wezel, 1971) or with marine conditions (e.g. Rouchy, 1976) and then evolved to hyperhaline conditions. For Rosell et al. (1998) the primary selenitic crystals on the top of each cycles reflect marine conditions, whereas Butler et al. (1995) considered them as salt-lake deposits. Londeix et al. (2007) suggested that the pollen content of the clay layer, preceding the last gypsum bed of the different cycles at Eraclea Minoa, indicates variable conditions that vary from distal to coastal. The base of the UE is marked by an unconformity (Decima and Wezel, 1973; Butler et al., 1995; Garcia-Veigas et al., 1995). The UE lie on the salt in the distal part of the basin, whereas towards the proximal parts it shows onlap terminations on the underlying unit (ie. LE and/or CdB), where the terrigenous content decreases and becomes enriched in coarser material, due to changes in the fluvial discharge and drainage (Roveri et al., 2008).
- **Arenazzolo member:** this unit overlays the UE and is topped by the Pliocene marking the Messinian/Zanclean contact. It comprises a stratified arkosic sand with alternating thin layers of different grain-size which yielded a well-diversified fauna corresponding to brackish-water ostracods species (Lago Mare), mostly of Paratethyan origin (Bonaduce and Sgarrella, 1999; Rouchy and Caruso, 2006). Some authors distinguished the Lago Mare unit from the Arenazzolo member with the later lying unconformably on the earlier (Cita and Colombo, 1979; Bache et al., 2012). According to these authors there is a transition in the depositional environment from brackish shallow-water conditions during the Lago Mare to a high-energy littoral environment. Above the Arenazzolo lies unconformably the Trubi Formation that reflects open deep-water condition as shown by foraminiferal fauna (Cita and Colombo, 1979; Pierre et al., 2006) and dinoflagellate cyst flora (Londeix et al., 1999, 2007). Bache et al. (2012) suggested a 2 step reflooding after the MSC acme in order to explain these transitions.

In this paper, for our comparison with the CMD record, we will be focusing mainly on the Caltanissetta Basin where most of the stratigraphic models of the MSC are based on (Fig. 4). In particular we will consider the geometries, facies, distribution and thickness of the MSC units.

3. Data and methods

In this study we use a series of 2-D seismic reflection profiles covering the whole BP area with the highest density of data in the CMD compared to the other sub-basins (Fig. 2). Part of this dataset consists of low-resolution seismic lines including old oil industry data that has been recently re-processed, provided by Spectrum Company, with a standard processing flow until pre-stack time migration. Other old non-reprocessed seismic data was also provided by the Instituto Geologico y Minero de Espana (IGME). The high-resolution seismic lines are mainly covering the CMD and have been acquired during the SIMBAD survey (Maillard and Gaullier, 2013). High- and low-resolution lines were crossed for a better recognition, interpretation and mapping of the MSC units and surfaces.

The interpretation of the profiles was performed using the software Petrel® by Schlumberger®. Analysis of the seismic profiles following a seismic stratigraphic procedure in terms of reflection terminations, erosional truncations, onlaps, downlaps and configurations, allowed the identification of seismic units and their boundaries (Mitchum and Vail, 1977). The seismic horizons were then exported in digital format and imported to the geographic information system QGIS for the mapping of the MSC markers.

For the MSC seismic units and surfaces we adopt the nomenclature proposed by Lofi et al. (2011a, b).

The mean acoustic velocities used for the time-depth conversion and thickness estimates are: 1500 m/s for the seawater; 2300 m/s for the

Pliocene-Quaternary sequence derived from detailed curves based on wells (Maillard et al., 2014; Driussi et al., 2015 and references therein); 4500 m/s for the MSC pre-halitic unit (bedded units BU1 and BU2), based on the sonic log data tied to seismic profiles from Ochoa et al. (2015); 4780 m/s for the salt unit, based on laboratory measurements done on samples of halite from the MSC salts from Sicily published by Samperi et al. (2020); 3500 m/s for the MSC post-halitic bedded unit (BU3) assuming that it contains more terrigenous sediments than the pre-halitic bedded units (see results and discussion for more details).

4. Results: MSC markers of the CMD/BP

Seismic units and their bounding surfaces are well expressed and preserved in the CMD (Fig. 5B and C). Four MSC seismic units and several conformable or unconformable bounding surfaces were identified from high-resolution seismic profile's interpretation, based on their seismic facies and on their geometrical and seismo-stratigraphic positions and relationships. They are described hereafter.

- **Bedded unit 1 (BU1):** this unit is widespread, mainly on the present-day shelves and slopes of the BP, ranging from a minimum present-day depth of ~170 m below sea level beneath the shelves to a maximum of ~1200 m beneath Mallorca slope (Figs. 3A and 5C, SP, 2077). Its extension has been underestimated in previous studies (Driussi et al., 2015; Ochoa et al., 2015), as our new seismic dataset shows its wider presence on the Alicante shelf and on the shelf between Menorca and Mallorca islands. On oil industry profiles, BU1 is contained in 1 or 2 reflections, whereas on high resolution seismic profiles, it is made of up to 8, medium to high-amplitude, relatively low frequency, reflections (Fig. 6D–F). In the proximal domain, BU1 is overlain by the lower Pliocene unit and underlain by pre-MSC units (Fig. 5A, SP 791 to 1266; Fig. 5C, SP 1 to 662), respectively made of very low and low amplitude reflections. In more distal domains, BU1 is overlain by another MSC unit (BU3, described later in this section) and still underlain by pre-MSC sedimentary unit (Fig. 5A, SP 146 to 791; Fig. 5B, SP 150 to 833; Fig. 5C, SP 1016 to 2077).

The upper boundary of BU1 is marked by a regional erosional surface (TES or IES) (Fig. 5A, SP 791 to 1266; Fig. 5C, SP 309 to 2077; Fig. 6D–F)

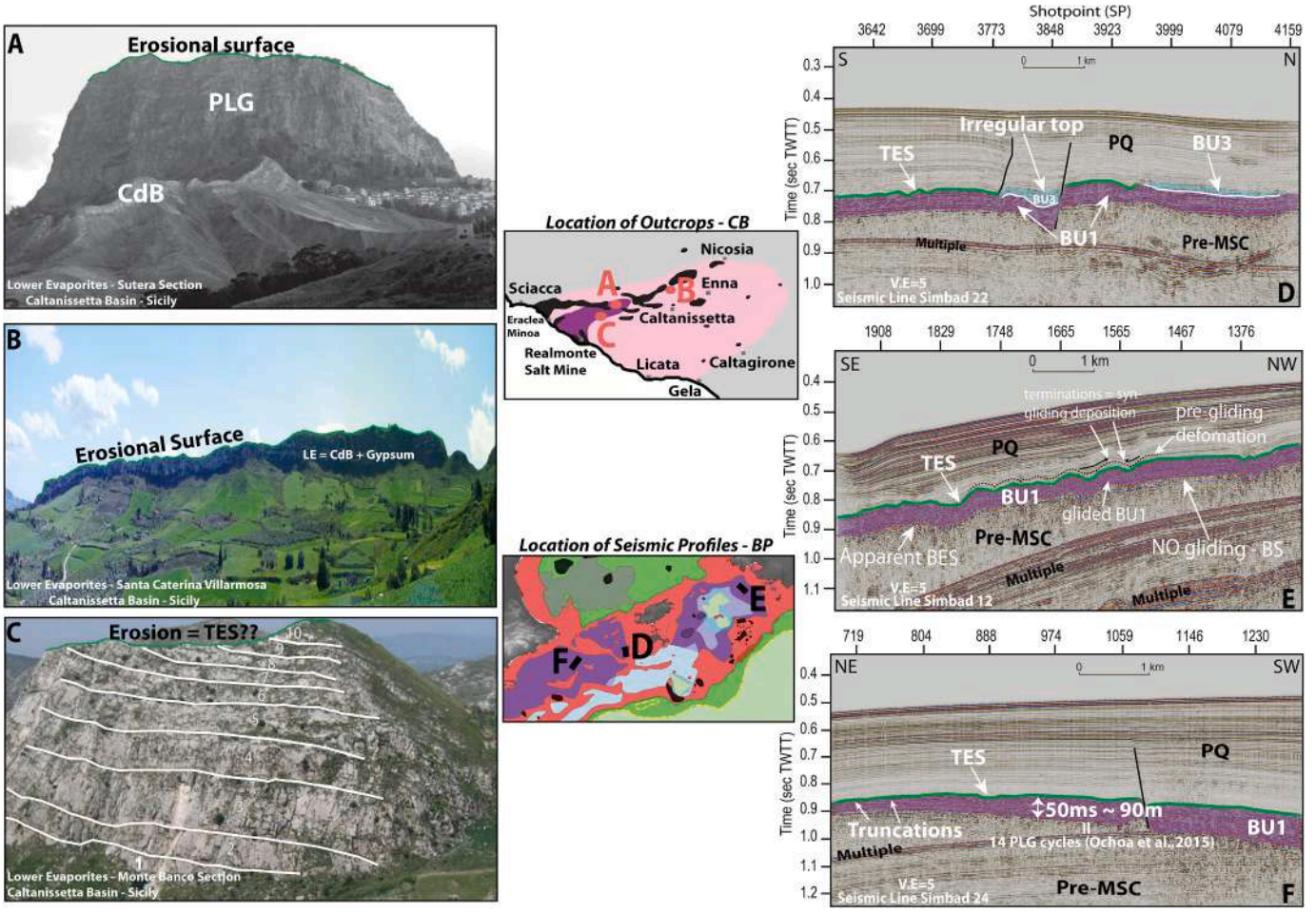

Fig. 6. Figure illustrating the comparison between the Lower Evaporites (LE) and Bedded Unit 1 (BU1) in CB and BP, respectively, both belonging to stage 1 of the MSC. A: Lower evaporites section in Sutera (CB – Sicily) showing a Primary Lower Gypsum (PLG) eroded at the top by an erosional surface (TES?) (modified from Manzi et al., 2011). B: Section of Santa Caterina Villarmosa showing the LE unit, cut by an erosional surface. C: Monte Banco section made of up to 10 PLG cycles eroded at the top (modified from Bonanni, 2018). See Fig. 4D for the legend of the outcrops' location map. D: Interpreted part of seismic profile Simbad 22 showing the bedded facies of BU1 on the southern slope of Ibiza, where it is truncated at the top by the TES. Here another MSC bedded unit (BU3) appears to lie locally above BU1. The irregular top of BU3 is probably due to syn-depositional faulting. E: Part of interpreted seismic profile Simbad 12 showing different facies of BU1: its facies appears perfectly bedded when undeformed, whereas its facies becomes more chaotic when deformed by gliding. Note that the gliding affecting the unit is post MSC, which means it could not be compared to the RLG. F: Part of seismic profile Simbad 24 located on the Alicante Shelf of south-east Spain, showing BU1 abruptly truncated at the top and thinning due to erosion towards the NE. Note that the seismic facies and the thickness of BU1 is similar in all sub basins in the BP, suggesting that it is everywhere made of stage 1 PLG cycles truncated at the top. See Fig. 3A for the legend of the seismic profiles' location map.

evidenced by truncated reflections (Fig. 6F). This erosion locally draw ~10–30 ms TWTT deep V to U-shaped incisions (Fig. 5C, SP ~1500). The lower boundary of BU1 is generally concordant with the underlying pre-MSC units (BS), except locally, where the unit is internally deformed with an apparently unconformable base, probably due to seismic artefacts (Fig. 6E). Both the upper and the lower boundaries show an abrupt amplitude change, evidencing high impedance contrasts between the BU1 and the overlying Pliocene and underlying pre-MSC units (Fig. 5 A-C and 6 D-E).

BU1 is characterized by several internal seismic facies alternating high amplitude continuous parallel reflections (bedded facies) (Fig. 6 D and F; Fig. 6E, SP 1376 to 1565) and medium amplitude deformed reflections (chaotic facies), observed especially on the slopes (Fig. 6E; SP 1565 to 1908). Reflection free facies is also locally found.

The thickness of BU1 is relatively constant along the BP (Fig. 6D–F), with an average thickness of ~110 m. It is thinner (~60 m; Fig. 5E) near the coastline of Mallorca, between Palma and Campos Basins, as a result of the partial erosion of the unit. W here not/slightly eroded or deformed, BU1 reaches a thickness of up to ~130 m on the slopes (Fig. 6E, SP 1467). BU1 is however, most of the times, absent on the shelves where only the MES is observed (Figs. 3A and 4A; Fig 5E, SP 1230). BU1 apparently thins out downslope (Fig. 5A, SP 592 to 1150), but its lateral continuity is unclear (Fig. 7E). On the seismic profile Simbad 14 (Fig. 5A) however, it seems continuous downslope.

- **Bedded unit 2 (BU2):** on oil industry seismic profiles it appears as a single reflection. On high-resolution profiles, it consists of up to 5 medium-to high-amplitude, relatively low frequency reflections. BU2 is overlain by the salt unit (see description of this unit later in this section) in the depocenters (Fig. 5B, SP, 1836 to 4497; Fig. 5C, SP 2784 to 4198; Fig. 5D, SP, 1943 to 3331), whereas on the slopes, where there's no salt, it is lying below another MSC unit, labelled BU3 (Fig. 5B, SP 833 to 1823; Fig. 5C, SP 4198 to 5259). BU2 is everywhere lying above pre-MSC sediments (Fig. 5B–D).

In relatively proximal zones, the upper boundary of BU2 appears to be an erosional surface with some incisions (~5–10 ms TWTT; Fig. 9, SP 991), whereas in the deeper depocenters it is conformable with the overlying salt unit (Fig. 5B, SP, 1836 to 2842). The lower boundary of BU2 is concordant with the pre-MSC units, but the low acoustic impedance contrast between those units makes it difficult to firmly identify the base of BU2.

The internal reflection pattern of BU2 is characterized by parallel reflections laterally continuous in the distal domain but their lateral continuity weakens moving towards the proximal domain (Fig. 5C, SP 2430 to 5259).

The maximum observed thickness of BU2 is 50 ms TWTT (~110 m–65 m depending on its internal lithology; see discussion for details). This thickness may be underestimated as the base of BU2 is uncertain, especially in the deepest part of the CMD. The lateral extent of BU2 toward shallower depths is also not clear and its relationship with the BU1 not properly imaged (Fig. 7E). It is not excluded that BU2 could be the distal continuation (and thus the time equivalent) of BU1, accumulated in a more proximal domain (Figs. 5C and 9A), but additional profiles would be needed to confirm this geometry.

Fig. 5C (SPs, 2077 to 2430; SP 5259) features an approximately 1.5 km wide mounded structure overlain by the lower Pliocene and apparently lying directly above BU1 (Fig. 7E). It is observed on the borders of the depocenter, close to the pinch-out out of BU3. The seismic signal around this feature does not allow us to figure out if any of the BUs has onlap termination on the structure. Onlap terminations and draping of the base reflections of the PQ unit on this mounded feature can be observed.

- **Salt unit:** this unit displays a classical dominantly reflection free (transparent) facies (e.g. Lofi et al., 2011a, b). Internal low-amplitude low-frequency continuous reflections are commonly observed in this unit (Fig. 5B, SP 2570 to 3177; Fig. 5C, SP 3137 to 3844; Fig. 9A, SP 1274 to 2122). The salt unit lies everywhere below BU3 and above BU2 (Fig. 4 B and C; Fig. 5B–E).

The upper boundary of the salt is an unconformable surface marked by a truncation of the topmost internal reflections (Fig. 4 B and C; Fig. 9A). The base of the salt is clearly concordant with BU2.

Its maximum thickness is ~240 m, reached in the deepest part of the CMD.

The base of the salt (top BU2) remains locally uncertain because of the poor imaging below the salt on high-resolution seismic data, but crossing with confidential re-processed oil industry profiles confirmed its location at 1.8–1.9 s TWTT in the CMD (Fig. 5 B and C) and not deeper as questioned by Maillard et al. (2014). Toward the borders, the salt thins out as a wedge. Due to the ductile deformation of the salt, its pinch-out termination is often associated with listric faults and brittle deformation of the overlying BU3 and PQ units (Fig. 5B, SPs, 1836, 3177 and ~4250). These listric faults, together with the deformation of the units overlying the salt, suggest that originally the salt extension was locally wider, and that it later glided towards the depocenter, leading to formation of salt welds (Fig. 5C). Moreover, the current thinning of the salt (wedge geometry) towards the borders of the salt basin is not an expression of progressive onlap of younger layers. It results from an erosion evidenced by the truncation of the intra-salt reflections, more and more into deeper (older) levels towards the margin.

Seismic profile Simbad 13 shows that the top of the salt exhibits locally a concave U-shaped depression lying above down-warped internal seismic reflections (Fig. 5C, SP 3491). The relief extends for about 1.5 km horizontally along the seismic profile. Down-warped reflections are also observed in the BU3 and PQ deposits overlying the depression but the deformation is progressively attenuated upwards (Fig. 7D).

- **Bedded unit 3 (BU3):** on oil industry profiles it is made of 2 reflections, whereas on high resolution profiles it consists of up to 9 low-to medium-amplitude, high frequency reflections (Fig. 8F). BU3 is everywhere conformably overlain by the lower Pliocene. In proximal domains, it unconformably overlies either the MES (Fig. 5D, SP, 1943) or BU1 or BU2 (Fig. 5A and B). Internal reflections of BU3 show onlap terminations on the erosion surface (IES) bounding above BU1/BU2 (Fig. 8D and E). More distally, in the depocenters, BU3 conformably overlies the salt unit (Fig. 5 A-D and 8 D, E). On the border of the salt basin, BU3 is often affected by brittle deformation related to the ductile deformation of the underlying salt (Fig. 5C, SPs 2784 and 4198).

The spatial extent of BU3 is limited to some of the BP sub-basins (Fig. 3A). BU3 shows no lateral continuity or geometrical connection with the UU accumulated in the deeper basins surrounding the BP (Fig. 3A).

The internal facies of BU3 consists dominantly of parallel and clearly continuous reflections in the distal part of the CMD and Formentera Basin (Fig. 5 A-D and 8 F). It becomes hummocky and relatively chaotic towards the proximal areas (Fig. 8E). In shallower sub-basins, such as El Cid and Cogedor Basins, BU3 overlies BU1 and appears as a very thin unit, with less beddings and irregular top (Fig. 6D, SP 3848).

The thickness of BU3 is variable. In the CMD it reaches a maximum thickness of ~120 m in the structural lows and/or in flat regions at the foot of slopes (Fig. 8F). In the southwestern basins of the BP, e.g. El Cid Basin, BU3 appears very thin on high-resolution seismic lines and thus cannot be distinguished from BU1 on the low-resolution seismic lines. Consequently, its presence might be underestimated in the southwestern part of the BP, where we have scarce high-resolution seismic coverage (Fig. 3).

The PQ unit overlies BU3 in the distal domain (Fig. 5B–D). In proximal domains it overlies BU1 where present (Fig. 5E, SP 719 to

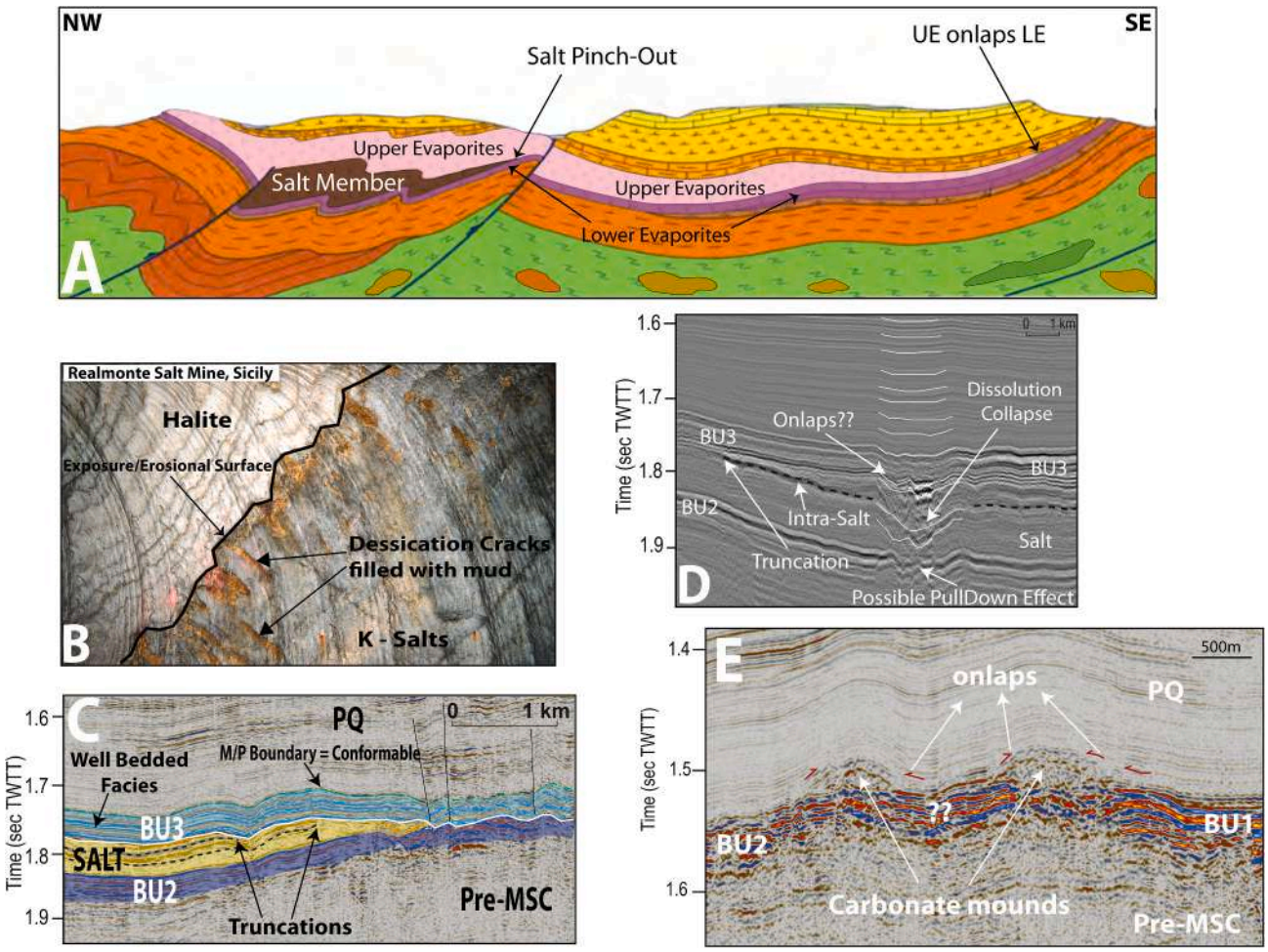

Fig. 7. Figure showing the geometrical settings and facies of the salt unit in CB and BP. A: Geological cross section between the towns of Caltanissetta and Enna in CB (position in Fig. 4D; modified from Carta Geologica Italiana, Caltanissetta, foglio 631, ISPRA, 1991). The section shows how the salt formation (here deformed by regional tectonics) belonging to the MSC is lying in between the lower and upper evaporites in the center of the section and it pinches-out in NW and SE directions, where the LE and UE become in contact. Note the onlap of the UE on the LE in the southeastern border of the basin. B: The MSC salt at the Realmonte Mine, CB, Sicily, showing an exposure surface at the top of the K–Mg salts with the desiccation cracks and the passage to halitic salts. C: Part of the seismic line Simbad 15 showing the truncation of the internal reflections at the top of the salt and illustrating an erosional surface which we interpret as an exposure surface or a dissolution surface in shallow water. Note how the salt unit in the BP, equivalent to CB's salt, is sandwiched between two other MSC units in the central basin: where the salt pinches-out, the underlying BU2 and overlying BU3 units become in contact. D: Zoom from seismic profile Simbad 13, showing a concave feature on the top of the salt, and associated down-wrapped reflections below and above, possibly related to salt dissolution at depth and associated cover collapse. E: Zoom showing the facies of the interpreted carbonate mounds (see text for details). It also shows the uncertainty about passage from BU1 to BU2.

1146) or the MES where BU1 is absent (Fig. 5D, SP 297; Fig. 5E, SP 1230). The basal part of the PQ unit is characterized everywhere on the BP by a very low amplitude reflectivity (Fig. 5 and 6D–F), except locally (e.g. Fig. 5B, SP 3845). The pattern of the basal reflections of the PQ unit in the CMD shows a clear sheet-like shape, draping the topography of the underlying Messinian units (Lüdmann et al., 2012). On the Mallorca slope it is deformed by the post-MSC gliding affecting BU1 (Fig. 6E; Maillard et al., 2014).

5. Interpretation/discussion

5.1. Sicily vs Balearic Promontory: depositional units, surfaces and geometries

Several sedimentary models were proposed to account for the MSC deposits observed in the Sicilian Basins (Fig. 4E–G), starting from the oldest models by Decima and Wezel (1971) and Garcia-Veigas et al. (1995), to more recent models by Rouchy and Caruso (2006) and Roveri et al. (2008). In all these models the depocenter of Caltanissetta Basin contains a halite unit sandwiched between two MSC units, the LE and the UE. Our seismic observations evidence that the MSC units in the BP, especially in the CMD, show a similar configuration: in the depocenter there is a salt unit (Fig. 4A) sandwiched between two other MSC units, BU2 below and BU3 above (Fig. 4 B, C).

The distribution of the MSC deposits in Sicily has been described schematically by Roveri et al. (2006) (Fig. 3D). In their model, only the marginal sub-basins such as Calatafimi Basin contain in situ PLG deposited in shallow context, whereas deeper basins such as Belice Basin contain only RLG (see section 3). The even deeper sub-basins of Caltanissetta are the only basins where salt and the upper evaporites are found (Figs. 3D and 4D). A very similar distribution is remarked in the BP, where the shallow perched sub-basins usually contain exclusively BU1, locally topped by a very thin BU3 with an irregular but non-erosional top (Fig. 6D). The deeper sub-basins (Formentera Basin; Fig. 5D and CMD; Fig. 5B and C) contain BU2 and a thick BU3, together with the salt unit in between (Fig. 3A).

Herein we discuss a possible analogy between Messinian Sicilian basins and B P sub-basins, assuming that the MSC seismic units of the BP, described in the previous section, could be the equivalent of the Sicilian MSC units described in section 2.2.

Observations of Messinian sub-basins from both BP and Sicily show a high analogy between the evaporitic units in terms of geometry, facies and distribution. In our comparison we will focus mainly on the CMD and CB.

5.1.1. Geometry similarities

a In the north-eastern part of the CB, seismic profiles imaging MSC sediments in a relatively undeformed or slightly deformed perched sub-basin (Fig. 9B and C), show that this depression has a concave-like geometry. The MSC unit is thicker in the depression's depocenter and includes salt, whereas towards the borders of the depressions, the salt pinches-out and there is a notable thinning of the MSC units. This geometry is very similar to the one observed in the CMD (Figs. 5C and 9A).

b The top of the PLG in Sicily is cut by a regional erosional surface in the shallower parts of the basins (Fig. 6A, C) and is locally overlain by the lower Pliocene Trubi Fm. Similarly, in the proximal part and the slopes of the BP, the top of BU1 is cut by a regional erosional surface (TES in Fig. 6E) and is overlain by the lowest Pliocene unit.

c Towards the depocenter, in the CB, the UE overly the LE and the contact between those 2 units is often marked by an erosional surface (Fig. 8A and B; and Roveri et al., 2019). In the distal areas of the BP, BU3 overlies BU1 and the contact between the two units is also erosional (IES in Fig. 8D and E).

d The MSC salt in the CB is lying between 2 units (i.e. LE and UE; Fig. 4 E-G and 7 A) and is found in the depocenters. Towards the margins, the salt unit pinches out where LE and UE become in contact along an erosional surface.Exactly the same configuration is observed in the C MD, where the MU is underlain by BU2 and overlain by BU3 in the depocenter (Fig. 5B and C). Toward the margin of the depression, the salt pinches out where BU2 and BU3 are in contact along an IES (Fig. 4B and C).

e In the depocenters of CB, the UE lie on the salt, where the transition is defined by a meter-thick laminar cumulate gypsum horizon (Fig. 4F). In a more proximal location, on the borders of the basin, clear onlap terminations of the UE against the LE (PLG and/or CdB) is observed (Fig. 8A and B; Decima and Wezel 1971; Rouchy and Caruso 2006; Roveri et al., 2008).A similar geometrical relationship exists in the CMD, where the post-salt BU3 lies above the salt unit

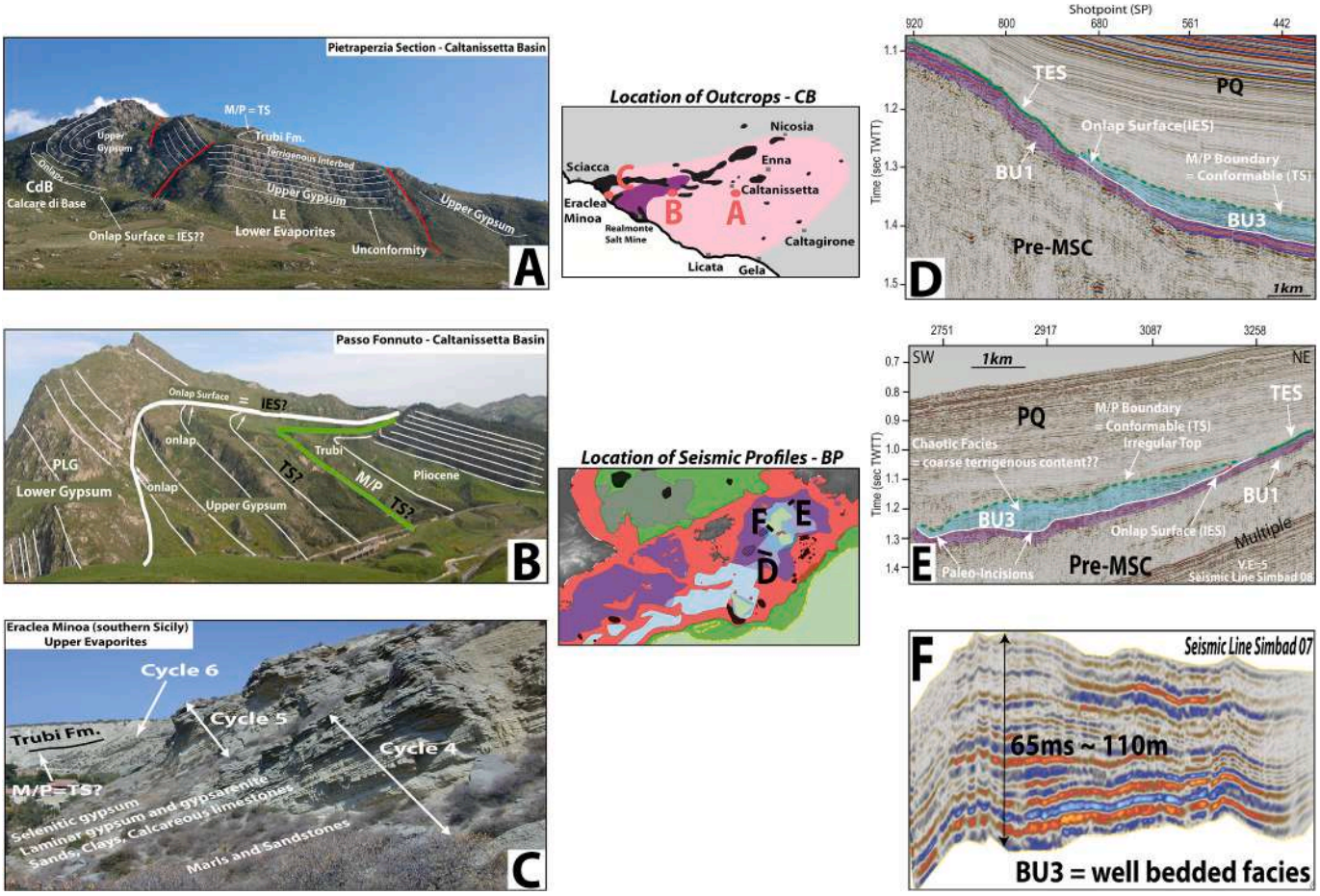

Fig. 8. Figure showing the similarities between UE and BU3 in CB and CMD, respectively. A: Pietraperzia section (central CB – Sicily); Deformed upper gypsum cycles with terrigenous content in the uppermost cycle, showing onlap termination on the CdB along an erosional surface IES. B: Passo Fonnuto section (CB – Sicily; modified from Roveri et al., 2019); UE onlapping LE along an erosional surface. Note that the lower Pliocene formation (Trubi) is conformable with the UE (TS?). C: The upper evaporites cycles of the Eraclea Minoa section (CB – southern Sicily); the cycles are made of selenitic and clastic gypsum intercalated with levels of marls, limestones and clays. This facies is considered to be the most complete and has been deposited in the depocenter of the CB. For the legend of the outcrops' location map see Fig. 4D. D: Zoom from seismic profile Simbad 14 showing the onlap of BU3 on BU1 along an erosional surface (IES) on the southern border of the CMD. Note the poor beddings of the horizons of the PQ unit and the continuous (conformable) transition from the MSC to PQ. E: Part of seismic line Simbad 08 showing the onlap geometry of BU3 on BU1 on the northern border of the CMD along an erosional surface (IES). Note how the IES is characterized by Messinian paleo-incisions whereas the top of BU3 is conformable with the PQ unit. BU3's facies is poorly bedded here probably due to coarse terrigenous content, explaining its thickening. F: Figure showing the perfectly bedded facies of BU3 in the deep depocenter of CMD where it reaches its maximum thickness. It's worth noticing how both BU3 and UE change their facies from the depocenter into the borders of the basins and how both units onlap an older MSC unit along an erosional surface.

(Fig. 4B and C) in the depocenter and onlaps BU1/BU2 (Fig. 5B, SPs 309 to 2077, and 4198 to 4905) in the proximal domains of the basin (Fig. 5A, SP 791; Fig. 5C, SPs ~800 and ~5100; Fig. 8D and E).

5.1.2. Facies similarities

a *PLG vs BU1*

The PLG in the CB has been described and correlated across the Mediterranean by Lugli et al. (2010). It consists of processional driven cycles of primary gypsum separated by shale horizons. Ochoa et al. (2015) demonstrated that the BU1 of the Elche sub-basin also corresponds to the PLG. It is made of cyclical gypsum/marl alternations (up to 14 cycles; Fig. 6F) and displays a bedded seismic facies (see section 4, BU1), as expected from such internal lithologies. This bedded seismic facies is typical of the BU1 and is observed at the scale of the promontory, suggesting that BU1 is the equivalent of the PLG everywhere on the BP, and not only in the Elche Basin. The erosional surface at the top of BU1 (Fig. 6D–F) supports for its interpretation.

b *RLG vs BU2*

The RLG in Sicily consist of resedimented gypsarenites, gypsum laminates, and PLG gypsum blocks. As already discussed in section 2.2, the origin of the large dislocated blocks of RLG in the C B is controversial. However, both interpretations of RLG blocks imply an active syn-tectonic activity in the basin for the block-sliding. This is not the case in the BP, where the syn and post-tectonic movements are relatively negligible. In the MSC records of the BP, we thus do not expect the presence of large olistostromes, which could have been at the origin of internal chaotic seismic facies as stated by Roveri et al. (2019). Thus, due to the geometrical position of BU2 below the salt, and the relatively continuous reflections it contains, it could be the equivalent of the RLG of CB made of gypsarenites and gypsum cumulates (sensu Rouchy and Caruso, 2006) resedimented from BU1 as well as primary. However, in the CMD, the relationship between BU1 and BU2 remains unclear. Both are clearly pre-dating the salt emplacement, and BU2 seems at least partly lateral time equivalent of BU1, but with a change in internal facies, that could be due to a change in the internal content in gypsum (Fig. 5 B, C). At this stage, a firm link between BU2 and RLG is difficult to establish.

c *Salt unit vs Halite*

The salt sequence in the CB consists mainly of Halite and K–Mg salts that show a clear shallowing upward trend until reaching an exposure erosional surface expressed by desiccation cracks (Fig. 7B; see section 3 and Lugli et al., 1999). In the CMD the salt sequence is characterized by a globally transparent seismic facies with internal reflections in its upper part (Fig. 4B and C; Fig. 7D). Those intra-salt reflections suggest that it is not made of pure/unique salt. The uppermost reflection is truncated abruptly at the top, which could be due to subaerial exposure or dissolution in shallow water. The erosional surface observed in the Realmonte mine of the CB (Fig. 7B) is found inside the salt unit and not at the top of it as in the salt observed in the CMD. The presence of a major erosion on the top of the salts in CB could not be excluded, as also described in the model of Decima and Wezel (1973) (Fig. 4E). In fact, there could be several minor erosional/exposure surfaces inside the salt unit of the CMD as well, with only the major one visible at a seismic scale.

d *UE vs BU3*

The thickness of the UE unit reaches its maximum in the depocenter of CB. Its sedimentary facies is characterized by thick mudstone, sandstone and marl intercalations (Fig. 8C; see section 2.2). Towards the margins of the basin this unit thins out until onlapping the LE, and the terrigenous layers tend to decrease and be rich in coarser material (Fig. 8A).This is an adequation with the characteristics of BU3. This unit reaches its maximum thickness in the distal part of the perched basins, especially in Formentera Basin and the CMD (Fig. 8F) and thins out towards the proximal part of the basins (Fig. 8D and E), where it onlaps the underlying unit. Moreover, the seismic facies of BU3 changes laterally from the distal to the proximal domains, passing from a well bedded horizontal unit (Figs. 4B and 8F) into a more discontinuous, less bedded one (Fig. 8E). This facies change could be due to the finer granulometry of the clastic intercalations between gypsum beds in the depocenter (shales to sandstone?) and coarser grain in more proximal context (conglomerates?).

5.2. CMD stratigraphy and relative chronology

In the offshore domain of the BP, ODP and DSDP scientific drillings do not exist. Oil industry drillings exist only on the Alicante shelf, on the southwestern part of the BP. They only offer borehole logs and cuttings providing discontinuous lithological record of the MSC depositional unit (Ochoa et al., 2015, 2018). Thus, the seismic method and onshore-offshore correlation approach are the only possible way to understand the history of deposition of the MSC deposits at a regional scale. Hereafter we discuss the significance and the chronology of the MSC units in the BP focusing on the CMD area based on the new interpretation of the seismic dataset. Most importantly, these units show similarity with the Sicilian CB (section 5.1).

BU1: based on the following observations, we interpret BU1 as corresponding to the Primary Lower Gypsum (PLG) deposited during the first stage of the MSC:

1 the proximal part of BU1 lies on a depth similar to the one of the PLG drilled onland in the Palma Basin (~120–200 m below sea level; Rosell et al., 1998; Garcia-Veigas et al., 2018). They also show similar thicknesses (80–90 m; Rosell et al., 1998);
2 the seismic facies of BU1 is everywhere similar (see section 4.1 and Fig. 6D–F) to the BU drilled on the Alicante shelf and interpreted as PLG (Ochoa et al., 2015), which suggests that the petro-physical characteristics of the unit are similar;
3 along the BP, BU1 is truncated almost everywhere by a regional erosional surface at the top, sometimes expressed by a valley-shaped incisions (Fig. 5C), suggesting a subaerial exposure of the unit during the MSC base level fall. This erosion could thus be the analog of the one at the top of the PLG in other peri-Mediterranean MSC basins (e.g. Sorbas and Appenines; Roveri et al., 2019; Roveri et al., 2001). The erosional top of the BU1 becomes less important moving distally, which could reflect a shorter exposure time for subaerial erosion in distal areas and progressive transition to subaqueous erosion towards more distal areas;
4 BU1 shows a high positive contrast in seismic impedance with the overlying PQ unit, suggesting BU1 is made of harder rocks than the marls above, in agreement with the presence of gypsum layers. BU1 locally shows internal reflection free facies (e.g. Fig. 5E, SP 719 to 804) possibly reflecting the presence of thick gypsum cycles such as cycles 3 to 5 that are, summed together, up to 60 m thick and that have been correlated on the Mediterranean scale (Lugli et al., 2010). This has been also hypothesized by Roveri et al. (2019) based on synthetic seismic models (see their Fig. 10).
5 BU1 is locally deformed, showing internal chaotic facies (Fig. 5C, SP 309), probably due to the gliding of the entire unit (Fig. 6E, SP 1565 to 1908), at the gypsum/pre-MSC interface. Since the deformation also affects the lowermost overlying Pliocene strata (Fig. 6E), the gliding occurred after the MSC. It could have been triggered by several factors, among which the increase in slope angle with time, as a result of margin subsidence, favored by the rheological contrast between the gypsum layers and underlying clastic sediments

(probably marls). Gliding along gypsum interfaces has also been described by Bourrillot et al. (2010) in the PLG of the Sorbas Basin. Locally, the internal chaotic facies could also be due to the presence of gypsum supercones similar to the one described in the PLG of Sorbas Basin (branching selenite facies, sensu Lugli et al., 2010).

Roveri et al. (2019) stated that BU1 in the CMD (SU) may correspond to chaotic deposits emplaced by gravity flows containing small to giant PLG gypsum blocks. We believe that their hypothesis is not correct, since RLG is known to be deposited in the second stage of the MSC, whereas the gliding affecting BU1 appears clearly to be post MSC (Fig. 6E). Moreover, the RLG is thought to be transported from margins and re-deposited basinwards (Roveri et al., 2008) which is not the case for BU1 which shows an in-situ (<1 km) gliding without transport and re-sedimentation. Moreover, except very little in the Palma Bay, no gypsum exists all around the CMD's margins, so there is no possible source that such RLG might derive from.

BU2: the relatively high amplitude of some internal reflections of BU2 (Fig. 5C, SP 4198 to 5259) suggests that this unit contains gypsum. Since the geometrical and temporal relationship between BU1 and BU2 is not clear, we consider hereafter two possible alternative interpretations for BU2:

- BU1 passes laterally to BU2 in the distal domain with a change in facies, and thus BU2 is the lateral and time equivalent of BU1, deposited in MSC stage 1. This is supported by several observations: 1- Locally, where BU1 is absent, we find BU2 currently lying at a depth that coincide with the depth of BU1; 2- No onlaps are observed between BU2 and BU1 and BU2 is never observed overlying BU1. In such case, several interpretations for BU2 are possible. It could be made of marls and thin carbonatic layers deposited in deep water conditions (equivalent in time to PLG being deposited in the shallower domain) in the distal parts of the basin, similar to the one locally described in the CB by Manzi et al. (2011). It could be also made of shales similar to the one described in other Messinian evaporitic basins such as the Piedmont Basin by Dela Pierre et al. (2011). However, such shales and/or marls have usually a very low sedimentation rate, especially in areas not very active tectonically. Considering the thickness of BU2 (maximum 65 m for such lithologies), it is unlikely that they could have been deposited during stage 1 of MSC (duration of 0.37 Ma). More in accordance with the observed seismic facies, BU2 could also be made of pelagic primary gypsum cumulates depositing on the deep sea-bottom as a snow fall (Warren, 2016) or on the shallower slopes and then resedimented in deeper areas (De Lange and Krijgsman, 2010). An alternation between gypsum cumulates and shales/marls is however not excluded. The downslope thinning of BU1 is compatible with what has been observed for the PLG in the Piedmont Basin by Dela Pierre et al. (2011).
- BU1 does not pass laterally to BU2, and BU2 is postdating BU1. This implies that BU2 is post-dating stage 1 of the crisis, emplaced probably in stage 2. The lateral discontinuity of the reflections of BU2 is the only observation that makes us doubt its continuity with BU1 (Fig. 5B, SP 833 and 5C, SPs 2430 and 5259). In this case, BU2 could be the product of erosion and re-sedimentation of BU1, possibly mixed with primary gypsum, as for the RLG in the CB (Roveri et al., 2008). In such a case, the absence of chaotic facies and diffractions in BU2 would imply that this type of RLG is likely made of gyps-turbidites rather than dislocated PLG blocks.

Moreover, we interpret the mounded features described in section (4.1.1, BU2; Fig. 5C) as microbial carbonate mounds. These carbonates could have been formed at the paleo-shoreline during the maximum retreat of the sea-level in the acme of the MSC (during deposition of BU3?), and they could be the equivalent of CdB or CdB1 described by Caruso et al. (2015) and Manzi et al. (2011), respectively. Similar isolated carbonate buildups with identical seismic facies has also been identified and described elsewhere in non-MSC contest (e.g. offshore Ireland by Hovland (2008), their Fig. 5.3; offshore Philippines by Burgess et al. (2013), their Figs. 6B and 8C; and offshore Indonesia by Ruf et al. (2012), their Fig. 7).

Salt: the salt unit fills the deepest parts of the CMD where it reaches its maximum thickness (~240 m). Salt tectonics is clearly observed (Fig. 4 B, C; Fig. 9A). The MU post-dates BU1 and BU2 since it is lying above the latter and pinches out laterally on it, which proves that it was deposited in a later stage of the MSC.

We propose that the salt unit is likely mainly made of halite like the other MSC salt bodies in the Mediterranean (e.g. CB, Lugli et al., 1999; Levant Basin, Feng et al., 2016). The continuous reflections in this unit might reflect a change in lithology from halite to Mg- and K-salts, as observed in the Sicilian salt (Decima and Wezel, 1971) of the CB. This would indicate increased brine concentration toward the top of the unit and could be related to a shallowing upward depositional environment (Lugli et al., 1999).

Clastic intercalations have also been encountered in the MSC halite (MU) of the Levant Basin in the eastern Mediterranean. The intercalations consist of layers of claystones (Gvirtzman et al., 2013; Feng et al., 2016) and/or argillaceous diatomites (Meilijson et al., 2019). Such intercalations give birth to high-amplitude high-frequency reflections on the seismic profiles (Feng et al., 2016, their Fig. 2), due to the important change in the petrophysical characteristics between halite and clay/diatomites. In the CMD, the internal reflections in the salt unit are characterized by low-amplitude and low-frequency. This suggest only a slight change in the petrophysical characteristics of the material at the origin of the reflection and we thus believe that the reflections within the salt of the CMD are due to change of evaporite type rather than to the presence of clastics.

The top of the salt in the CMD is marked by the truncation of intra-salt reflections (Fig. 7 B, C). This erosional unconformity could be originated either by salt dissolution in under-saturated shallow diluted water (Kirkham et al., 2020) or by subaerial exposure (Ryan, 1978), both processes requiring a significant base level drop. Toward the borders of the salt basin, the fact that the truncation cuts into progressively older stratigraphic levels in the landward direction suggests that the salt was initially extending further landward and has subsequently been removed from shallower depths, supporting the hypothesis of an important drop in the base level associated with this erosional event. A similar geometry has been evidenced on in the deep Levant basin where intra-salt truncations are interpreted as of subaerial origin (Ryan, 1978), in agreement with the presence further north of fluvial deposits deposited at the top of the salt (Madof et al., 2019). In the CMD, we interpret the down-warped seismic reflections in the salt and overlying units as possibly imaging a solution-subsidence structure (Fig. 7D) related to the dissolution of the subjacent salt. Overburden collapse structures related to dissolution of subjacent evaporites have also been evidenced in the Levant Basin by Bertoni and Cartwright (2005) and Hübscher et al. (2009). We tentatively suggest that in the CMD, such a dissolution may have been initiated during the lowstand phase contemporaneous with the erosion of the top of the salt.

BU3: We interpret this unit as the possible equivalent of the stage 3 MSC deposits of the CB (upper evaporites and the Lago Mare sub-stages). In the CMD, the important acoustic impedance contrast between BU3 and the overlying lower PQ unit (probably marls and calcisiltites similar to the lower Pliocene unit of Palma Basin; Capo and Garcia 2019) reflects an important change in lithology. The internal stacking bedded facies of BU3 in the depocenter of the CMD (Fig. 8F) is coherent with an internal lithology consisting of alternations of gypsum and fine clastic sediments similar to the one described at Eraclea Minoa in CB. The low frequency characterizing the facies of BU3 (Fig. 8F) with respect to the high frequency ones encountered in BU1 could reflect the thicker layers of clastics included in it, similar to the clays and marls of the UE (Fig. 8C). If present, the Lago Mare phase representing the end of the

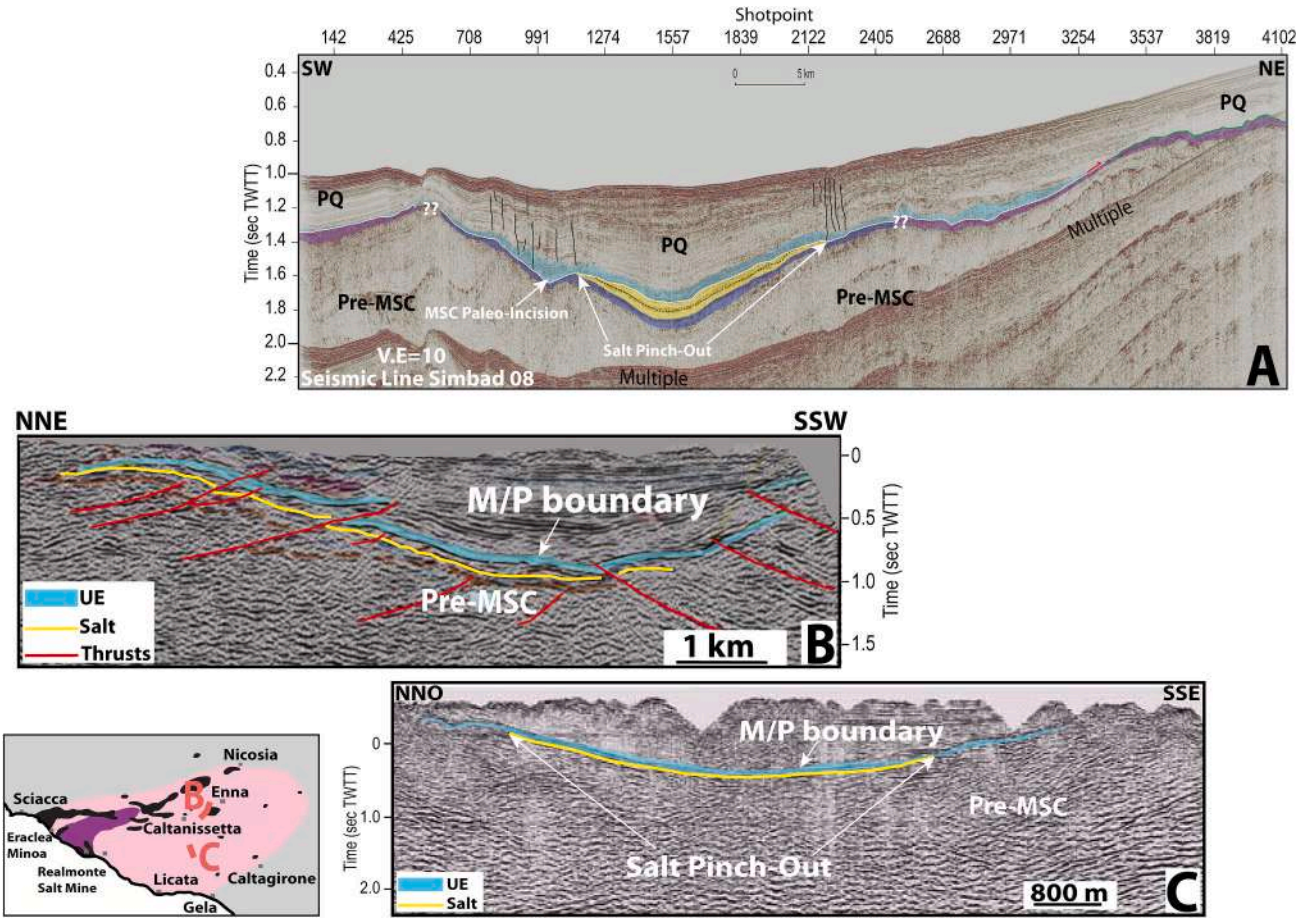

Fig. 9. Interpreted profiles from both BP and CB showing the similarity in the shape and geometry of the sub-basins, especially here where a post-MSC flexure affected locally the CMD. A: Seismic profile Simbad 08 crossing the CMD from the southern to the northern part through the depocenter (position and legend in Fig. 5). Note that the salt is exclusively found in the deepest part of the CMD, whereas to the borders it pinches-out. B: Onland seismic profile near Capodarso (CB – Sicily, modified from Catalano et al., 2013). C: Onland seismic profile in the central part of CB (modified from Catalano et al., 2013). See Fig. 4D for the legend of the location map. Note how in both the CMD and CB, the MSC sediments are contained in a concave-shaped depression with only the deepest part containing salt.

MSC could be contained in the uppermost reflection of BU3 or included in the lowermost PQ horizon due to its reduced thickness.

The aggrading pattern of BU3 suggests that, following the erosion of the top salt layer under lowered base-level, BU3 deposited in a topographic low forming a perched lake system. The onlap of the internal reflection of BU3 on the margin may reflect a rise in base-level, as the sediments infill the lake and the mean shoreline of the perched basin shoals through aggradation. This is in accordance with what proposed for the UE of the CB by Butler et al. (1995).

Similarly to the centi-metric to deci-metric scale erosions described in the UE in CB due to the precession driven sea-level oscillations (Rouchy and Caruso, 2006), internal erosions within BU3 might exist, but they are not visible at the seismic scale. The top of BU3 marking the Miocene-Pliocene (M/P) boundary is conformable in the CMD with no evidence of erosion on the seismic scale (Fig. 4B and C) suggesting that the perched lake always remained under water. The M/P boundary in CB is however interpreted as unconformable (see section 2.2, Arenazzolo member; Cita and Colombo, 1979). In other shallower sub-basins in the BP, a very thin BU3 appears locally. The irregular top could be due to mild syn-tectonic faulting affecting the unit (Fig. 6D).

5.3. *Proposed depositional scenario in the CMD and associated regional consequences*

Maillard et al. (2014) proposed several possible correlations between the different MSC markers of the BP, extending from onshore to offshore. Roveri et al. (2019) subsequently adapted one of the proposed scenarios (see their Fig. 14) to fit their 3-stages model. However, two crucial features were not considered in both previous works: the BU2 lying below the salt and the clear erosional surface truncating the top of salt.

The approach that we use in this work and the similarities that we discussed between the CMD and CB, help us not only to constrain our understanding of the MSC in the BP, but also it could be a reciprocal way to answer some uncertainties about the MSC in CB.

Thus, hereafter we propose a new scenario (Fig. 10) for the MSC in the CMD following our observations, interpretation, and comparisons and adapting the CIESM (2008) time chronological model for the MSC:

- MSC stage 1 (5.97–5.60 Ma): during this stage, the Terminal Carbonate Complex (TCC), known also as Santanyi Limenstones formation, has been deposited on Mallorca carbonate shelves contemporaneously with the Primary lower gypsum (PLG) in the Palma de Mallorca Basin (Mas and Fornos, 2012). Concurrently in the CMD, BU1 and BU2, which we interpret respectively as PLG and primary gypsum cumulates/marls, were deposited in continuity with the PLG of the southern Spanish basins, as equivalent to the lower evaporites unit of the Sicilian MSC basins.
- MSC stage 2 (5.60–5.55 Ma): in this stage, a major base-level drop took place. The TCC and PLG already deposited in the proximal parts were undergoing an important subaerial erosion. In the depocenter of the CMD, salt bodies deposited in the 2 disconnected depressions, probably from high-concentrated salt brines. At the acme of this

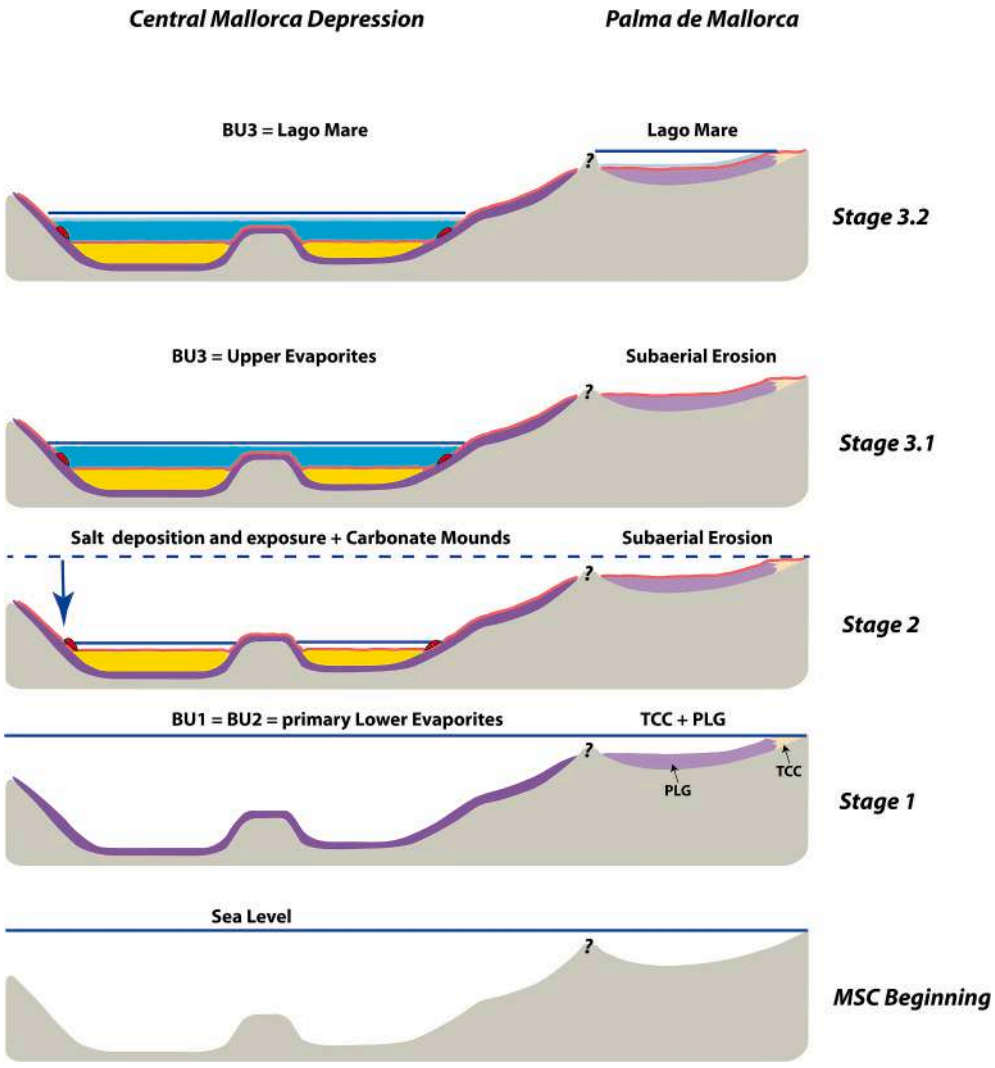

Fig. 10. Proposed scenario of the MSC event in the CMD inspired from our new dataset interpretation and comparison with CB, adapting the consensus age model of the CIESM (2008). Stage 1: deposition of BU1 and BU2 contemporaneously with TCC and PLG in the Palma Basin. Stage 2: Major sea-level drawdown during which the units deposited in stage one, were exposed to intense subaerial erosion and the deposited in the depocenter from two high-concentrated salt brines. At the paleo-shoreline, mounded carbonates equivalent to the CdB1 in CB probably formed in this stage. Stage 3.1: Deposition of BU3 in the CMD, the equivalent of the Upper Gypsum of the CB. Stage 3.2: Deposition of Lago Mare sediments from brackish-water lakes formed at different heights, probably due to increased rivers run-off.

stage, the base-level dropped until the exposure and erosion of the top of the salt layers, marked by the truncation of the salt's internal reflections. This erosion could also be due to dissolution of salt in shallow waters. The salt's internal reflections likely reflect the change in the salt facies from halitic to kainite salts. At the border of the depression, microbial carbonate mounds deposited near to the paleo-shoreline. This carbonate formation might have continued also in the next stage. Moreover, the bidirectional truncation of the intra-salt reflections suggests that salt may have been eroded on the higher flanks of the basin during the acme of the crisis, and then re-deposited in the deepest part of the depocenter. This observation is evidenced by the presence of a pure salt transparent facies above the intra-salt reflections in the depocenter. This process might have acted also in the salts of CB, where above the desiccation cracks at the top of the K and Mg-salts lies a pure halitic unit that could have deposited due to the washing of salts deposited initially at the flanks of the depression and re-deposition in the deepest area, as also indicated by the Strontium isotopes values in this unit (Garcia-Veigas et al., 2018).

- MSC stage 3 (5.55–5.33): during this stage, BU3 was deposited in the CMD. The bedded pattern of BU3 and its seismo-stratigraphic position suggest that it is likely affected by cyclicity similar to the one observed in the UE of the CB. The Lago Mare deposits were deposited in the CMD, as well as in the Palma Basin at the very end of this stage. This could have happened perched brackish lakes lying at different levels and that has received high volumes of fresh water from increased water runoff, similar to what observed in the Arenazzolo member in CB by Cita and Colombo (1979).

Onland Mallorca, as well as at Eraclea Minoa in CB, the M/P boundary is marked by an unconformity reflecting the return of normal marine conditions following the Zanclean re-flooding. This unconformity is not observed on the seismic scale in the CMD. The lowermost horizons of the PQ unit in the CMD drapes the slopes up to the shelves, which indicate deposition in normal marine conditions (Fig. 5C; Lüdmann et al., 2012).

6. Conclusions

The interpretation of a wide seismic reflection dataset covering the Balearic Promontory area allowed us to refine the mapping of the MSC unit's distribution and establish better the connection between the MSC sub-basins of the promontory. We were able to distinguish 4 different seismic units based on their seismic facies and on their geometrical and stratigraphic relationships. Those seismic units are, from the oldest to the most recent one: BU1/BU2, Salt Unit and BU3. They are very well defined in the Central Mallorca Depression, where we have the best coverage among the basins in terms of density of high-resolution seismic data. The settings and geometrical relationships of the MSC units in the CMD show a strong analogy with the MSC sediments of the Caltanissetta

Basin in Sicily, in terms of stratigraphic geometries, distribution and facies. In both the BP and Sicily, the Messinian deposits are situated in a series of sub-basins that were lying during the late Messinian at different water depths. The deepest basins accumulated a relatively thin (~300–500 m) salt unit, sandwiched between two other MSC units. The comparison of the MSC units in the BP with the ones outcropping in Sicily allowed to constrain and propose a new 3-stages scenario for the MSC in the CMD.

- The BU1 deposited first and is interpreted as equivalent to the bottom growth selenitic PLG found in CB and correlated on the Mediterranean scale (Lugli et al., 2010). BU1 is widespread and its present-day depth below sea level ranges from ~170 m beneath the shelves to ~1200 m beneath the Mallorca slope. The erosion surface at the top of BU1, restricted to the borders of the basins, is interpreted as of subaerial origin, when the base level of the Mediterranean was lowered.
- The unit BU2, lying below the salt unit, is here considered as the temporal lateral equivalent of BU1 made of primary gypsum cumulates (snowfall) possibly mixed with clastic sediments.
- Following the deposition of BU1/BU2, the salt unit filling the depocenters of the CMD accumulated in topographic lows forming perched sub-basins. It likely started depositing in relatively deep water and ended in shallow water. This unit is interpreted as halite rich where displaying transparent seismic facies, while the internal reflections may reflect K and Mg- salts. Their truncation strongly suggests a phase of subaerial exposure or dissolution under shallow water-column, contemporaneous with the Mediterranean base level lowering during the second phase of the crisis. The geometry of the intra-salt reflection truncations suggests that the salt layer in its entirety may have deposited higher up on the margin slopes before removal by erosion/dissolution.
- Above the salt, the youngest MSC unit, BU3, is considered as the equivalent of the Sicilian Upper Evaporites, including the Lago Mare event. This last deposited in perched lakes fed with fresh waters and topographically disconnected from the surrounding deeper basins in which the base level was lower.

This work suggests that the CMD can be considered as an undeformed analog of the Sicilian CB. During the MSC drawdown phase, temporary perched lakes developed in sub-basins forming topographic depressions lying at intermediate water depths. During the acme of the crisis, the sea-level drawdown was thus important enough to disconnect the BP sub-basins from the Valencia Basin and the rest of the Mediterranean.

The Sicilian MSC records (salt and the evaporites lying below and above it), classically provide key chronostratigraphic constrains for the MSC scenarios. They are often considered as representative of the deep basin records in particular to date the onset of the salt deposition at the Mediterranean scale. In our study, the clear absence of geometrical connection between the thin salt bodies found in the BP sub-basins and the thick salt layer from the deep Liguro-Provencal and Algerian Basins, however, indicate that salt deposition in perched basins is thus not necessarily contemporaneous with the deep basin salt, as also suggested recently by Meilijson et al. (2019) based on Eastern Mediterranean deep basin drillings. For the same reason, we also question the age and the origin of the thick, so-called, Lower Unit (LU), considered sometimes to be the equivalent of the outcropping Lower Evaporites. The CB salt and more generally its MSC records, should thus be used with care when trying to extrapolate the chrono-stratigraphy to the deep basin records.

The change in facies between BU1 and BU2 described in this work and interpreted respectively as the passage at a certain depth range from primary bottom growth selenitic PLG to primary pelagic snowfall gypsum cumulates, is of an important significance as it might represent the maximum depth of formation of bottom growth selenitic gypsum in a non silled basin. In the BP, this depth is clearly exceeding the 200 m threshold proposed by Lugli et al. (2010) and is in agreement with the work of Ochoa et al. (2015), thus suggesting that PLG is not strictly related to shallow silled basins.

Table of acronyms. Acronyms used in this paper for the study area and the MSC units, with the references to the origin of each term, where applicable.

	Term	Acronym	Reference
	Messinian Salinity Crisis	MSC	
	Balearic Promontory	BP	
	Central Mallorca Depression	CMD	
	Caltanissetta Basin	CB	
Offshore MSC units	Bedded Unit	BU	Lofi et al. (2011a, b)
	Lower Unit	LU	
	Mobile Unit	MU	
	Upper Unit	UU	
	Complex Unit	CU	
Onshore MSC units	Lower Evaporites	LE	Decima and Wezel (1973)
	Upper Evaporites	UE	
	Primary Lower Gypsum	PLG	Roveri et al. (2006)
	Resedimented Lower Gypsum	RLG	
	Calcare di Base	CdB	Ogniben (1957)
	Terminal Carbonate Complex	TCC	Esteban (1979)
Onshore/Offshore MSC surfaces	Margin Erosional Surface	MES	Lofi et al. (2011a, b)
	Bottom Erosional Surface/ Bottom Surface	BES/BS	
	Intermediate Erosional Surface/Intermediate Surface	IES/IS	
	Top Erosional Surface/Top Surface	TES/TS	

Author contribution statement

The reference author Fadl Raad performed the seismic interpretation, mapping and writing of the manuscript. Johanna Lofi and Agnes Maillard contributed, supervised and planned the interpretation, development and planning of the work, as well as, contributed to the writing and revision of the manuscript. Athina Tzevahirtzian and Antonio Caruso helped in the interpretation of the outcrops and onland geology of Sicily and provided field photos, as well as in the reading and revision of the manuscript.

Funding information

This research is carried out under the SALTGIANT ETN, a European project funded by the European Union's Horizon 2020 research and innovation program under the Marie Sklodowska-Curie grant agreement number 765256.

Declaration of competing interest

The authors declare that they have no known competing financial interests or personal relationships that could have appeared to influence the work reported in this paper.

Acknowledgments

SALTGIANT ESRs and PIs are all thanked for the numerous exchanged discussions and comments during workshops, courses and fieldtrips. We are grateful to Francesco Dela Pierre for inspiring discussions on the Messinian Salinity Crisis.

William B.F. Ryan is warmly thanked for the extremely constructive review and comments that significantly improved this manuscript. We

also acknowledge the anonymous reviewer and the editor for their helpful comments. Spectrum and Western Geco Companies are thanked for providing seismic data that helped in the interpretation and mapping. Hanneke Heida is thanked for the proofreading of the final manuscript.

Appendix A. Supplementary data

Supplementary data to this article can be found online at https://doi.org/10.1016/j.marpetgeo.2020.104777.

References

Acosta, J., Canals, M., Lopez-Martinez, J., Munoz, A., Herranz, P., Urgeles, R., Palomo, C., Casamor, J.L., 2002. The Balearic Promontory geomorphology (western Mediterranean): morphostructure and active processes. Geomorphology 49, 177–204.

Albanese, C., Sulli, A., 2012. Backthrusts and passive roof duplexes in fold-and-thrust belts: the case of Central-Western Sicily based on seismic reflection data. Tectonophysics 514, 180–198.

Bache, F., Popescu, S.M., Rabineau, M., Gorini, C., Suc, J.P., Clauzon, G., et al., 2012. A two-step process for the reflooding of the Mediterranean after the Messinian Salinity Crisis. Basin Res. 24 (2), 125–153.

Baron, A., Gonzalez, C., 1985. Correlation and geometry of the Messinian facies on the oriental edge of the Palma plain (Island of Mallorca). In: 6th European Regional Meeting Lleida, p. 5 (April).

Bertoni, C., Cartwright, J.A., 2006. Controls on the basinwide architecture of late Miocene (messinian) evaporites on the levant margin (eastern mediterranean). Sediment. Geol. 188, 93–114.

Bertoni, C., Cartwright, J.A., 2005. 3D seismic analysis of circular evaporite dissolution structures, Eastern Mediterranean. J. Geol. Soc. 162 (6), 909–926.

Bonaduce, G., Sgarrella, F., 1999. Paleoecological interpretation of the latest Messinian sediments from southern Sicily (Italy). Memor. Soc. Geol. Ital. 54, 83–91.

Bonanni, D.M., 2018. The messinian salinity crisis. The Mystery of the Vanished Sea 2. https://en.calameo.com/read/0051898537b317dcb2d2c.

Bouillin, J.-P., Durand-Delga, M., Olivier, P., 1986. Betic-Rifian and Tyrrhenian Arcs: distinctive features, genesis and development stages. In: Wezel, F.C. (Ed.), The Origin of Arcs. Elsevier, pp. 281–304.

Bourillot, R., Vennin, E., Rouchy, J.M., Blanc-Valleron, M.M., Caruso, A., Durlet, C., 2010. The end of the Messinian Crisis in the western Mediterranean: insights from the carbonate platforms of south-eastern Spain. Sediment. Geol. 229, 224–253.

Burgess, P.M., Winefield, P., Minzoni, M., Elders, C., 2013. Methods for identification of isolated carbonate buildups from seismic reflection data. AAPG Bull. 97 (7), 1071–1098.

Butler, R.W.H., Lickorish, W.H., 1997. Using high-resolution stratigraphy to date fold and thrust activity: examples from the Neogene of south-central Sicily. J. Geol. Soc. 154 (4), 633–643.

Butler, R.W., Lickorish, W.H., Grasso, M., Pedley, H.M., Ramberti, L., 1995. Tectonics and sequence stratigraphy in Messinian basins, Sicily: constraints on the initiation and termination of the Mediterranean salinity crisis. Geol. Soc. Am. Bull. 107 (4), 425–439.

Butler, R.W.H., McCLelland, E., Jones, R.E., 1999. Calibrating the duration and timing of the Messinian salinity crisis in the Mediterranean: linked tectono-climatic signals in thrust-top basins of Sicily. J. Geol. Soc. Lond. 156, 827–835.

Camerlenghi, A., Accettella, D., Costa, S., Lastras, G., Acosta, J., Canals, M., Wardell, N., 2009. Morphogenesis of the SW Balearic continental slope and adjacent abyssal plain, Western Mediterranean Sea. Int. J. Earth Sci. 98 (4), 735.

Cameselle, A.L., Urgeles, R., 2017. Large-scale margin collapse during Messinian early sea-level drawdown: the SW Valencia trough, NW Mediterranean. Basin Res. 29, 576–595.

Capó, A., Garcia, C., 2019. Basin filling evolution of the central basins of Mallorca since the Pliocene. Basin Res. 31 (5), 948–966.

Caruso, A., Pierre, C., Blanc-Valleron, M.M., Rouchy, J.M., 2015. Carbonate deposition and diagenesis in evaporitic environments: the evaporative and sulphur-bearing limestones during the settlement of the Messinian Salinity Crisis in Sicily and Calabria. Palaeogeogr. Palaeoclimatol. Palaeoecol. 429, 136–162.

Caruso, A., Rouchy, J.M., et al., 2006. The upper gypsum unit. In: Roveri, M. (Ed.), Post-Congress FieldTrip of the RCMNS Interim Colloquium (Parma, 2006, Acta Naturalia de "L'Ateneo Parmense", vol. 42, pp. 157–168.

Catalano, R., Di Stefano, P., Sulli, A., Vitale, F.P., 1996. Paleogeography and structure of the central mediterranean: sicily and its offshore area. Tectonophysics 260, 291–323.

Catalano, R., Valenti, V., Albanese, C., Accaino, F., Sulli, A., Tinivella, U., et al., 2013. Sicily's fold–thrust belt and slab roll-back: the SI. RI. PRO. seismic crustal transect. J. Geol. Soc. 170 (3), 451–464.

CIESM, 2008. The Messinian salinity crisis from mega-deposits to microbiology. In: Briand, F. (Ed.), A consensus report, in 33ème CIESM Workshop Monographs, 33. CIESM, 16, bd de Suisse, MC-98000, Monaco, pp. 1–168.

Cita, M.B., Colombo, L., 1979. Sedimentation in the latest messinian at Capo rossello (sicily). Sedimentology 26 (4), 497–522.

Clauzon, G., Suc, J.-P., Gautier, F., Berger, A., Loutre, M.F., 1996. Alternate interpretation of the Messinian salinity crisis, controversy resolved? Geology 24, 363–366.

Clauzon, G., Suc, J.-P., Popescu, S.-M., Marunt, EanuM., Rubino, J.-L., Marinescu, F., Melinte, M.C., 2005. Influence of the mediterranean sea-level changes over the dacic basin (eastern paratethys) in the late Neogene. The mediterranean Lago Mare facies deciphered. Basin Res. 17, 437–462.

De Lange, G.J., Krijgsman, W., 2010. Messinian salinity crisis: a novel unifying shal-low gypsum/deep dolomite formation mechanism. Mar. Geol. 275, 273–277.

Decima, A., McKenzie, J.A., Schreiber, B.C., 1988. The origin of "evaporative" limestones: an example from the Messinian of Sicily (Italy). J. Sediment. Petrol. 58, 256–272.

Decima, A., Wezel, F.C., 1971. Osservazioni sulle evaporiti Messiniane della Sicilia centromeridionale. Riv. Mineraria Sicil. 130–134, 172–187.

Decima, A., Wezel, F.C., 1973. Late Miocene evaporites of the central Sicilian basin, Italy. In: Ryan, W.B.F., Hsü, K.J., et al. (Eds.), Initial Rep. Deep Sea Drill. Prog., vol. 13. U. S. Govt. Printing Office, Washington, pp. 1234–1240.

Dela Pierre, F., Bernardi, E., Cavagna, S., Clari, P., Gennari, R., Irace, A., Lozar, F., Lugli, S., Manzi, V., Natalicchio, M., Roveri, M., Violanti, D., 2011. The record of the Messinian salinity crisis in the Tertiary Piedmont Basin (NW Italy): the Alba section revisited. Palaeogeogr. Palaeoclimatol. Palaeoecol. 310, 238–255.

Driussi, O., Maillard, A., Ochoa, D., Lofi, J., Chanier, F., Gaullier, V., et al., 2015. Messinian Salinity Crisis deposits widespread over the Balearic Promontory: insights from new high-resolution seismic data. Mar. Petrol. Geol. 66, 41–54.

Durand-Delga, M., Freneix, S., Magné, J., Méon, H., Rangheard, Y., 1993. La série saumâtre et continentale d'âge Miocène moyen et supérieur d'Eivissa (ex-Ibiza, Baléares). Acta. Geol. Hisp. Barcelona 28 (1), 33–46.

Escutia, C., Maldonado, A., 1992. Palaeogeographic implications of the messinian surface in the Valencia trough, northwestern mediterranean sea. Tectonophysics 203 (1–4), 263–284.

Esteban, M., 1979. Significance of the upper Miocene coral reefs of the western mediterranean. Palaeogeogr. Palaeoclimatol. Palaeoecol. 29, 169–188.

Feng, Y.E., Yankelzon, A., Steinberg, J., Reshef, M., 2016. Lithology and characteristics of the Messinian evaporite sequence of the deep Levant Basin, eastern Mediterranean. Mar. Geol. 376, 118–131.

García-Veigas, J., Ortí, F.J., Rosell, L., Ayora, C., Rouchy, J.M., Lugli, S., 1995. The Messinian salt of the Mediterranean: geochemical study of the salt from the central Sicily basin and comparison with the Lorca Basin (Spain). Bull. Soc. Geol. Fr. 166, 699–710.

García-Veigas, J., Cendón, D.I., Gibert, L., Lowenstein, T.K., Artiaga, D., 2018. Geochemical indicators in western mediterranean messinian evaporites: implications for the salinity crisis. Mar. Geol. 403, 197–214.

Gelabert, B., Sàbat, F., Rodríguez-Perea, A., 1992. A structural outline of the serra the tramontana of majorca (balearic islands). Tectonophysics 203, 167–183.

Ghielmi, M., Minervini, M., Nini, C., Rogledi, S., Rossi, M., 2013. Late Miocene-Middle Pleistocene sequences in the Po Plain-Northern Adriatic Sea (Italy): the stratigraphic record of modification phases affecting a complex foreland basin. Mar. Petrol. Geol. 42, 50–81.

Grasso, M., Butler, R.W.H., 1991. Tectonic controls on the deposition of late Tortonian sediments in the Caltanissetta Basin of central Sicily. Mem. Soc. Geol. Ital. 47, 313–324.

Grossi, F., Gliozzi, E., Anadon, P., Castorina, F., Voltaggio, M., 2015. Is cyprideis agrigentina Decima a good paleosalinometer for the messinian salinity crisis? Morphometrical and geochemical analyses from the Eraclea Minoa section (sicily). Palaeogeogr. Palaeoclimatol. Palaeoecol. 419, 75–89.

Gvirtzman, Z., Manzi, V., Calvo, R., Gavrieli, I., Gennari, R., Lugli, S., et al., 2017. Intra-Messinian truncation surface in the Levant Basin explained by subaqueous dissolution. Geology 45 (10), 915–918.

Gvirtzman, Z., Reshef, M., Buch-Leviatan, O., Ben-Avraham, Z., 2013. Intense salt deformation in the Levant basin in the middle of the messinian salinity crisis. Earth Planet Sci. Lett. 379, 108–119.

Haq, B., Gorini, C., Baur, J., Moneron, J., Rubino, J.L., 2020. Deep mediterranean's messinian evaporite giant: how much salt? Global Planet. Change 184, 103052.

Henriquet, M., Dominguez, S., Barreca, G., Malavieille, J., Monaco, C., 2020. Structural and tectono-stratigraphic review of the Sicilian orogen and new insights from analogue modeling. Earth Sci. Rev. 103257.

Hovland, M., 2008. Deep-water Coral Reefs: Unique Biodiversity Hot-Spots. Springer Science & Business Media.

Hsü, K., Ryan, W.B.F., Cita, M., 1973a. Late Miocene desiccation of the mediterranean. Nature 242, 240.

Hsü, K.J., Cita, M.B., Ryan, W.B.F., 1973b. The origin of the Mediterranean evaporites. In: Ryan, W.B.F., Hsü, K.J., Cita, M.B. (Eds.), Initial Reports of the Deep Sea Drilling Project 13, Part 2. U.S. Government Printing Office, Washington D.C., pp. 1203–1231

Hsü, K.J., Montadert, L., Bernoulli, D., Cita, M.B., Erikson, A., Garrison, R.E., Kidd, R.B., Melieres, F., Muller, C., Wright, R.H., 1978. Initial Report of Deep Sea Drilling Project. Mediterranean Sea. U.S. Government Printing Office, Washington, DC, p. 42.

Hübscher, C., Tahchi, E., Klaucke, I., Maillard, A., Sahling, H., 2009. Plate and salt tectonic control of fluid dynamics in the Latakia and Cyprus Basin, eastern Mediterranean. Tectonophysics 470, 173–182.

IGME (Date accessed/Publication date). BDMIN. Base de Datos de Recursos minerales ©Instituto Geológico y Minero de España (IGME). Retrieved from: http://doc.igme.es/bdmin/.

ISPRA. Istituto Superiore per la Protezione e la Ricerca Ambientale. Carta Geologica D'italia, 1:50000, Foglio 631. http://www.artasicilia.eu/old_site/web/carg/index.html.

Kastens, K.A., Mascle, J., Auroux, C., Bonatti, E., Broglia, C., Channell, J., Curzi, P., Emeis, K., Glacon, G., Hasegawa, S., Hieke, W., Mascle, G., McCoy, F., McKenzie, J., Mendelson, J., Muller, C., Rehault, J.-P., Robertson, A., Sartori, R., Sprovieri, R., Torii, M., 1988. ODP leg 107 in the Tyrrhenian Sea: insights into passive margin and back-arc basin evolution. Geol. Soc. Am. Bull. 100, 1140–1156.

Kirkham, C., Bertoni, C., Cartwright, J., Lensky, N.G., Sirota, I., Rodriguez, K., Hodgson, N., 2020. The demise of a 'salt giant'driven by uplift and thermal dissolution. Earth Planet Sci. Lett. 531, 115933.

Krijgsman, W., Fortuin, A.R., Hilgen, F.J., Sierro, F.J., 2001. Astrochronology for the Messinian Sorbas Basin (SE Spain) and orbital (precessional) forcing evaporite cyclicity. Sediment. Geol. 140, 43–60.

Krijgsman, W., Hilgen, F.J., Raffi, I., Sierro, F.J., Wilson, D.S., 1999b. Chronology, causes and progression of the Messinian salinity crisis. Nature 400 (6745), 652.

Krijgsman, W., Hilgen, F.J., Marabini, S., Vai, G.B., 1999a. New paleomagnetic and cyclostratigraphic age constraints on the Messinian of the Northern Apennines (Vena del Gesso Basin, Italy). Mem. della So. Geol. Ital. 54, 25–33.

Lezin, C., Maillard, A., Odonne, F., Colinet, G., Chanier, F., Gaullier, V., 2017. Tectono-sedimentary Evolution of the Miocene-Pliocene Series of Ibiza: New Onshore Evidence of the Messinian Salinity Crisis. IAS Octobre 2017 Toulouse.

Lickorish, W.H., Grasso, M., Butler, R., Argnani, A., Maniscalco, R., 1999. Structural styles and regional tectonic setting of the "Gela Nappe" and frontal part of the Maghrebian thrust belt in Sicily. Tectonics 18 (4), 655–668.

Lofi, J., 2018. Seismic atlas of the messinian salinity crisis markers in the mediterranean sea. Mem. Soc. Geol. fr., n.s., 2018, t. 181, and Commission of the Geological Map of the World 2, 72. https://doi.org/10.10682/2018MESSINV2.

Lofi, J., Déverchère, J., Gaullier, V., Gillet, H., Gorini, C., Guennoc, P., Loncke, L., Maillard, A., Sage, F., Thinon, I., 2011a. Seismic atlas of the "messinian salinity crisis" markers in the mediterranean and black seas. Comm. Geol. Map World Mem. SoC. Géol. de France, Nouvelle Sér. 72.

Lofi, J., Gorini, C., Berné, S., Clauzon, G., Tadeu Dos Reis, A., Ryan, W.B.F., Steckler, M., 2005. Erosional processes and paleo-environmental changes in the western gulf of lions (SW France) during the messinian salinity crisis. Mar. Geol. 217, 1–30.

Lofi, J., Sage, F., Déverchère, J., Loncke, L., Maillard, A., Gaullier, V., et al., 2011b. Refining our knowledge of the Messinian salinity crisis records in the offshore domain through multi-site seismic analysis. Bull. Soc. Geol. Fr. 182 (2), 163–180.

Londeix, L., Benzakour, M., De Vernal, A., Turon, J.L., Suc, J.P., 1999. Late Neogene dinoflagellate cyst assemblages from the strait of sicily, central mediterranean sea: paleoecological and biostratigraphical implications. The Pliocene: Time Change 65–91.

Londeix, L., Benzakour, M., Suc, J.P., Turon, J.L., 2007. Messinian palaeoenvironments and hydrology in Sicily (Italy): the dinoflagellate cyst record. Geobios 40 (3), 233–250.

Lüdmann, T., Wiggershaus, S., Betzler, C., Hübscher, C., 2012. Southwest Mallorca Island: a cool-water carbonate margin dominated by drift deposition associated with giant mass wasting. Mar. Geol. 307, 73–87.

Lugli, S., Manzi, V., Roveri, M., Schreiber, B.C., 2010. The Primary Lower Gypsum in the Mediterranean: a new facies interpretation for the first stage of the Messinian salinity crisis. Palaeogeogr. Palaeoclimatol. Palaeoecol. 297, 83–99.

Lugli, S., Schreiber, B.C., Triberti, B., 1999. Giant polygons in the Realmonte mine (agrigento, sicily); evidence for the desiccation of a messinian halite basin. J. Sediment. Res. 69 (3), 764–771.

Madof, A.S., Bertoni, C., Lofi, J., 2019. Discovery of vast fluvial deposits provides evidence for drawdown during the late Miocene Messinian salinity crisis. Geology 47 (2), 171–174.

Maillard, A., Gaullier, V., Lézin, C., Chanier, F., Odonne, F., Lofi, J., 2020. New onshore/offshore evidence of the messinian erosion surface from key areas: the ibiza-balearic promontory and the orosei-eastern Sardinian margin. BSGF Eath Sci. Bull. 191, 9.

Maillard, A., Mauffret, A., 2006. Relationship between erosion surfaces and the late Miocene salinity crisis deposits in the Valencia Basin (northwestern mediterranean): evidence for an early sea-level drop. Terra. Nova 18, 321–329.

Maillard, A., Driussi, O., Lofi, J., Briais, A., Chanier, F., Hübscher, C., Gaullier, V., 2014. Record of the messinian salinity crisis in the SW Mallorca area (balearic promontory, Spain). Mar. Geol. 357, 304–320.

Maillard, A., Gorini, C., Mauffret, A., Sage, F., Lofi, J., Gaullier, V., 2006. Offshore evidence of polyphase erosion in the Valencia Basin (northwestern mediterranean): scenario for the messinian salinity crisis. Sediment. Geol. 188, 69–91.

Maillard, Lenoir Agnès, Gaullier, Virginie, 2013. SIMBAD Cruise, RV Téthys II. https://doi.org/10.17600/13450010.

Manzi, V., Gennari, R., Hilgen, F., Krijgsman, W., Lugli, S., Roveri, M., Sierro, F.J., 2013. Age refinement of the Messinian salinity crisis onset in the Mediterranean. Terra. Nova 25 (4), 315–322.

Manzi, V., Gennari, R., Lugli, S., Persico, D., Reghizzi, M., Roveri, M., Schreiber, B.C., Calvo, R., Gavrieli, I., Gvirtzman, Z., 2018. The onset of the Messinian salinity crisis in the deep Eastern Mediterranean basin. Terra. Nova 30, 189–198.

Manzi, V., Gennari, R., Lugli, S., Roveri, M., Scafetta, N., Schreiber, B.C., 2012. High-frequency cyclicity in the Mediterranean Messinian evaporites: evidence for solar–lunar climate forcing. J. Sediment. Res. 82 (12), 991–1005.

Manzi, V., Lugli, S., Roveri, M., Charlotte Schreiber, B., 2009. A new facies model for the Upper Gypsum of Sicily (Italy): chronological and palaeoenvironmental constraints for the Messinian salinity crisis in the Mediterranean. Sedimentology 56 (7), 1937–1960.

Manzi, V., Lugli, S., Roveri, M., Dela Pierre, F., Gennari, R., Lozar, F., et al., 2016. The Messinian salinity crisis in Cyprus: a further step towards a new stratigraphic framework for Eastern Mediterranean. Basin Res. 28 (2), 207–236.

Manzi, V., Lugli, S., Roveri, M., Schreiber, B.C., Gennari, R., 2011. The messinian CdB (sicily, Italy) revisited. Geol. Soc. Am. Bull. 123, 347–370.

Mas Gornals, G.Y., Fornós Astó, J.J., 2012. La Crisis de Salinidad del Messiniense en la cuenca sedimentaria de Palma (Mallorca, Islas Baleares); The Messinian Salinity Crisis Record in the Palma basin (Mallorca, Balearic Islands). Geogaceta 52, 57–60.

Mas, G., Fornós, J.J., 2013. Late messinian Lago Mare deposits of the island of Mallorca (western mediterranean). Implications on the MSC events. In: Neogene to Quaternary Geological Evolution of Mediterranean, Paratethys and Black Sea. Abstracts Book. 14th RCMNS Congress, 8-12 September 2013, Istanbul. Turkey, p. 210.

Mascle, G., Mascle, J., 2019. The Messinian salinity legacy: 50 years later. Mediterranean Geosci. Rev. 1–11.

Meilijson, A., Hilgen, F., Sepúlveda, J., Steinberg, J., Fairbank, V., Flecker, R., Waldmann, N.D., Spaulding, S.A., Bialik, O.M., Boudinot, F.G., 2019. Chronology with a pinch of salt: integrated stratigraphy of Messinian evaporites in the deep East-ern Mediterranean reveals long-lasting halite deposition during Atlantic connectivity. Earth Sci. Rev. 194, 374–398.

Mitchum Jr., R.M., Vail, P.R., 1977. Seismic Stratigraphy and Global Changes of Sea Level: Part 7. Seismic Stratigraphic Interpretation Procedure: Section 2. Application of Seismic Reflection Configuration to Stratigraphic Interpretation.

Montadert, L., Sancho, J., Fial, J.-P., Debysser, J., 1970. – De l'âge tertiaire de la série salifère responsable des structures diapiriques en Méditerranée occidentale (Nord-Est des Baléares). C.R. Acad. Sci., Paris 271, 812–815.

Ochoa, D., Sierro, F.J., Hilgen, F.J., Cortina, A., Lofi, J., Kouwenhoven, T., Flores, J.A., 2018. Origin and implications of orbital-induced sedimentary cyclicity in Pliocene well-logs of the Western Mediterranean. Mar. Geol. 403, 150–164.

Ochoa, D., Sierro, F.J., Lofi, J., Maillard, A., Flores, J.A., Suárez, M., 2015. Synchronous onset of the Messinian evaporite precipitation: first Mediterranean offshore evidence. Earth Planet Sci. Lett. 427, 112–124.

Odonne, F., Maillard, A., Lézin, C., Chanier, F., Gaullier, V., Guillaume, D., 2019. Large-scale boudinage of late Miocene platform series triggered by margin collapse during the messinian salinity crisis (Ibiza island, Spain). Mar. Petrol. Geol. 109, 852–867.

Ogniben, L., 1957. Petrografia della Serie Solfifera Siciliana e considerazioni geologiche relative. Mem. Descrit. Carta Geol. Ital. 33, 275.

Pedley, H.M., Maniscalco, 1999. Lithofacies and faunal succession (faunal phase analysis) as a tool on unravelling climatic and tectonic signals in marginal basins; Messinian (Miocene), Sicily. J. Geol. Soc. Lond. 156, 855–863.

Pellen, R., Aslanian, D., Rabineau, M., Suc, j., Gorini, C., Leroux, E., et al., 2019. The messinian Ebro river incinsion. Global Planet. Change 181, 102988.

Perri, E., Gindre-Chanu, L., Caruso, A., Cefalà, M., Scopelliti, G., Tucker, M., 2017. Microbial-mediated pre-salt carbonate deposition during the Messinian salinity crisis (Calcare di Base fm., Southern Italy). Mar. Petrol. Geol. 88, 235–250.

Pierre, C., Caruso, A., Blanc-Valleron, M.M., Rouchy, J.M., Orzsag-Sperber, F., 2006. Reconstruction of the paleoenvironmental changes around the miocene–pliocene boundary along a west–east transect across the mediterranean. Sediment. Geol. 188, 319–340.

Pomar, L., Ward, W.C., Green, D.G., 1996. Upper Miocene reef complex of the llucmajor area, Mallorca, Spain.). In: Franseen, E., Esteban, M., Ward, W.C., Rouchy, J.M. (Eds.), Models for Carbonate Stratigraphy from Miocene Reef Complexes of Mediterranean Regions. Soc. Econ. Paleontol. Mineral., Concepts in Sedimentology and Palaeontology Serie, vol. 5, pp. 191–225.

Roca, E., 2001. The northwest-Mediterranean Basin (Valencia trough, gulf of lions and liguro-provencal basins): structure and geodynamic evolution. In: Ziegler, P.A., Cavazza, W., Robertson, A.F.H. (Eds.), Peri-tethysmemoir, IGCP 369: Peri Tethyan Rift/Wrench Basins and Passive Margins. Mem. Mus. Natl. Hist. Nat., pp. 671–706. Paris.

Roca, E., Guimera, J., 1992. The Neogene structure of the eastern iberian margin: structural constraints on the crustal evolution of the Valencia trough (western mediterranean). Tectonophysics 203, 203–218.

Rosell, L., Orti, F., Kasprzyk, A., Playà, E., Marek Peryt, T., 1998. Strontium geochemistry of Miocene primary gypsum: messinian of southeastern Spain and sicily and badenian of Poland. J. Sediment. Res. 68, 63–79.

Rouchy, J.M., Caruso, A., 2006. The Messinian salinity crisis in the Mediterranean basin: a reassessment of the data and an integrated scenario. Sediment. Geol. 188, 35–67.

Rouchy, J.M., 1976. Mise en évidence de nannoplancton calcaire dans certains types de gypse finement lité (balatino) du Miocène terminal de Sicile et conséquences sur la genèse des évaporites méditerranéennes de cet âge. C. R. Acad. Sci. Paris 282, 13–16.

Rouchy, J.M., 1982. La genèse des évaporites messiniennes de Méditerranée. Bull. Muséum Natl. Hist. Natl. Paris, Sci. Terre 1–280.

Rouchy, J.-M., Saint-Martin, J.-P., 1992. Late Miocene events in the Mediterranean as recorded by carbonate-evaporite relations. Geology 20, 629–632.

Roveri, M., Bassetti, M.A., Ricci Lucchi, F., 2001. The Mediterranean messinian salinity crisis: an Apennine foredeep perspective. Sediment. Geol. 140, 201–214.

Roveri, M., Flecker, R., Krijgsman, W., Lofi, J., Lugli, S., Manzi, V., et al., 2014a. The Messinian Salinity Crisis: past and future of a great challenge for marine sciences. Mar. Geol. 352, 25–58.

Roveri, M., Gennari, R., Ligi, M., Lugli, S., Manzi, V., Reghizzi, M., 2019. The synthetic seismic expression of the Messinian salinity crisis from onshore records: implications for shallow-to deep-water correlations. Basin Res. 31 (6), 1121–1152.

Roveri, M., Lugli, S., Manzi, V., Schreiber, B.C., 2008. The shallow-to deep-water record of the Messinian salinity crisis: new insights from Sicily, Calabria and Apennine basins. In: CIESM Workshop Monographs, vol. 33, pp. 73–82.

Roveri, M., Lugli, S., Manzi, V., Gennari, R., Schreiber, B.C., 2014b. High-resolution strontium isotope stratigraphy of the Messinian deep Mediterranean basins: implications for marginal to central basins correlation. Mar. Geol. 349, 113–125.

Roveri, M., Manzi, V., Lugli, S., Schreiber, B.C., Caruso, A., Rouchy, J.-M., Iaccarino, S. M., Gennari, R., Vitale, F.P., Ricci Lucchi, F., 2006. Clastic vs. primary precipitated evaporites in the messinian Sicilian basins. RCMNS IC parma 2006 "the messinian

salinity crisis revisited II" post-congress field-trip. Acta Nat. Ateneo Parmense 42–4, 125–199.
Ruf, A.S., Simo, J.T., Hughes, T.M., 2012. Insights on Oligocene-Miocene carbonate mound morphology and evolution from 3D seismic data, East Java Basin, Indonesia. In: AAPG Annual Meeting, Long Beach, California, April 1-4, 2007. AAPG©2012.
Ryan, W.B., 1976. Quantitative evaluation of the depth of the western Mediterranean before, during and after the Late Miocene salinity crisis. Sedimentology 23 (6), 791–813.
Ryan, W.B., 1978. Messinian badlands on the southeastern margin of the Mediterranean Sea. Mar. Geol. 27 (3–4), 349–363.
Ryan, W.B., 2009. Decoding the Mediterranean salinity crisis. Sedimentology 56 (1), 95–136.
Ryan, W.B.F., Stanley, D.J., Hersey, J.B., Fahlquist, D.A., Allan, T.D., 1971. The tectonics and geology of the Mediterraneran Sea. In: Maxwell, A.E. (Ed.), The Sea. Wiley-Interscience, New York, pp. 387–492.
Sabat, F., Gelabert, B., Rodriguez-Perea, A., Giménez, J., 2011. Geological structure and evolution of Majorca: implications for the origin of the Western Mediterranean. Tectonophysics 510, 217–238.
Samperi, L., Giorgio, M., Kamaldeen, O., Alba, Z., Nicolas, W., Sabrina, N., Francesco, B., 2020. Estimation of the physical, petrophysical and mineralogical properties of Messinian salt rocks, Sicily: implications for multidisciplinary applications. Mar. Petrol. Geol. 112, 104032.
Schreiber, B.C., 1978. Environments of subaqueous gypsum deposition. In: Dean, E., Schreiber, B.C. (Eds.), Marine Evaporites, vol. 4. SEPM Short Course, pp. 43–73.
Schreiber, B.C., Friedman, G.M., Decima, A., Schreiber, E., 1976. Depositional environments of upper Miocene (messinian) evaporite deposits of the Sicilian basin. Sedimentology 23, 729–760.
Selli, R., 1960. Il Messiniano Mayer-Eymar 1867: Proposta di un neostratotipo. Museo Geologico, Giovanni Capellini. Servicio Wms Geode. Mapa Geológico Continuo de España a escala 1:50.000 ©Instituto Geológico y Minero de España (IGME) (Date accessed). Retrieved from. http://mapas.igme.es/gis/services/Cartografia_Geologica/IGME_Geode_50/MapServer/WMSServer.
Soria, J.M., Caracuel, J.E., Corbí, H., Dinarès-Turell, J., Lancis, C., Tent-Manclús, J.E., Viseras, C., Yébenes, A., 2008. The messinian–early Pliocene stratigraphic record in the southern Bajo Segura basin (betic Cordillera, Spain): implications for the mediterranean salinity crisis. Sediment. Geol. 203, 267–288.
Suc, J.-P., Violanti, D., Londeix, L., Poumot, C., Robert, C., Clauzon, G., Gautier, F., Turon, J.L., Ferrier, J., Chikhi, H., Cambon, G., 1995. Evolution of the messinian mediterranean environments: the Tripoli Formation at Capodarso (sicily, Italy). Rev. Palaeobot. Palynol. 87, 51–79.
Thinon, I., Guennoc, P., Serrano, O., Maillard, A., Lasseur, E., Rehault, J.P., 2016. Seismic markers of the messinian salinity crisis in an intermediate-depth basin: data for understanding the Neogene evolution of the Corsica Basin (northern Tyrrhenian Sea). Mar. Petrol. Geol. 77, 1274–1296.
Urgeles, R., Camerlenghi, A., Garcia-Castellanos, D., De Mol, B., Garcés, M., Vergés, J., et al., 2011. New constraints on the Messinian sealevel drawdown from 3D seismic data of the Ebro Margin, western Mediterranean. Basin Res. 23 (2), 123–145.
Vai, G.B., Lucchi, F.R., 1977. Algal crusts, autochthonous and clastic gypsum in a cannibalistic evaporite basin: a case history from the Messinian of Northern Apennines. Sedimentology 24 (2), 211–244.
Van Couvering, J.A., Castradori, D., Cita, M.B., Hilgen, F.J., Rio, D., 2000. The base of the zanclean stage and of the Pliocene series. Episodes 23 (3), 179–187.
Warren, J.K., 2016. Evaporites: A Geological Compendium. Springer.
Ziegenbalg, S.B., Brunner, B., Rouchy, J.M., Birgel, D., Pierre, C., Böttcher, M.E., Caruso, A., Immenhauser, A., Peckmann, J., 2010. Formation of secondary carbonates and native sulphur in sulphate-rich Messinian strata, Sicily. Sediment. Geol. 227, 37–50.